Palaeontology
The Palaeontological Association
Registered Charity No. 11683330

New information on the Jurassic lepidosauromorph Marmoretta oxoniensis

Journal:	*Palaeontology*
Manuscript ID	PALA-01-21-4988-OA.R1
Manuscript Type:	Original Article
Date Submitted by the Author:	29-Mar-2021
Complete List of Authors:	Griffiths, Elizabeth; University of Oxford, Earth Sciences Ford, David; University of the Witwatersrand, 2 Evolutionary Studies Institute; University of Oxford, Earth Sciences Benson, Roger; University of Oxford, Department of Earth Sciences Evans, Susan E.; University College London, Dept of Cell and Developmental Biology
Key words:	reptiles, lepidosaurs, skull, Jurassic, phylogeny

New information on the Jurassic lepidosauromorph *Marmoretta oxoniensis*

ELIZABETH F. GRIFFITHS[1*], DAVID P. FORD[1,2*], ROGER B.J. BENSON[1], SUSAN E. EVANS[3]

[1]Department of Earth Sciences, University of Oxford, South Parks Road, Oxford, OX1 3AN, UK; emails: elizabeth.griffiths@earth.ox.ac.uk (https://orcid.org/0000-0002-5241-1915), roger.benson@earth.ox.ac.uk (https://orcid.org/0000-0001-8244-6177)

[2] Evolutionary Studies Institute, University of the Witwatersrand, Johannesburg, South Africa (https://orcid.org/0000-0002-1771-6772)

[3] Research Department of Cell and Developmental Biology, University College London, London, WC1E 6BT, UK; email: s.e.evans@ucl.ac.uk (https://orcid.org/0000-0002-0799-4154)

* Joint first authors

ABSTRACT

The earliest known crown-group lepidosaurs are known from the Middle Triassic; however, their stem group is poorly sampled, with only a few representative fossils found. This is partly due to the small size and delicate bones of early stem-lepidosaurs (= non-lepidosaurian lepidosauromorphs), which make both preservation in the fossil record and subsequent discovery less likely. The Middle Jurassic lepidosauromorph *Marmoretta oxoniensis* Evans is re-examined using high-resolution µCT scanning to reveal parts of the skull anatomy that were previously unknown. These include a squamosal, postorbital, more complete parietal, pterygoids, and an articulated posterior section of the mandible. Some differences between this and other *Marmoretta* specimens were identified as a result, such as the arrangement of palatal teeth and the shape of the parabasisphenoid. The status of *Marmoretta* as a stem lepidosaur or stem squamate has been debated. To evaluate this, we tested the phylogenetic position of *Marmoretta* by including our new data in an adapted phylogenetic character matrix. We recover *Marmoretta* as a stem-lepidosaur and sister to *Fraxinisaura rozynekae.* Our findings support the hypothesis that both taxa belonged to a clade of non-lepidosaurian lepidosauromorphs that co-existed with lepidosaurs into the Middle Jurassic.

KEY WORDS: reptiles, lepidosaurs, skull, Jurassic, phylogeny.

LEPIDOSAURS comprise more than ~~10~~9,000 extant species (Jones *et al*. 2013~~Evans & Jones 2010~~), including squamates (lizards, snakes and amphisbaenians) and *Sphenodon*, the only extant rhynchocephalian. The earliest fossils of crown-group lepidosaurs occur in the early Middle Triassic (~240 million years ago; Jones *et al*. 2013), and their stem-lineage must extend back at least into the Permian, as indicated by the earliest occurrences of their extant sister taxon, Archosauromorpha e.g. Ezcurra *et al* (2014). However, the anatomy of stem-group lepidosaurs (i.e. non-lepidosaurian lepidosauromorphs) is not well known. Early stem-group lepidosaurs are currently represented by a few taxa primarily of early-middle Triassic age (Evans & Jones 2010), including the Early Triassic taxa *Paliguana whitei* (Carroll 1975) and *Sophineta cracoviensis* (Evans & Borsuk-Białynicka 2009), the Middle Triassic *Fraxinisaura rozynekae* (Schoch & Sues 2018), and, less certainly, the kuehneosaurs (specialised gliding reptiles with uncertain phylogenetic affinities, from the Early-Late Triassic; Evans & Jones 2010).

Marmoretta ~~*oxoniensis*~~ is a fossil lepidosauromorph from the Bathonian (166.1–168.3; Middle Jurassic; Gradstein *et al*. 2012) of the UK known from several localities in southern England and the Isle of Skye, Scotland (Evans 1991; Waldman & Evans 1994). It is also known from the late Jurassic of Portugal (Evans 1991). Most studies have considered *Marmoretta* as a stem-group lepidosaur (Schoch & Sues 2018), in which case it might represent a relict lineage, being significantly younger than other stem-group lepidosaurs. However, a recent phylogenetic study found it as a stem-group squamate (Simões *et al*. 2018), raising questions about its phylogenetic position. Nevertheless, *Marmoretta* has the potential to provide important anatomical data on deep lepidosaurian and lepidosauromorph divergences.

Most specimens of *Marmoretta* are fragmentary and disarticulated bones collected from screenwashing of bulk sediments (e.g. Evans 1991). However, specimens from the Isle of Skye include a semi-articulated partial skeleton (NMS G1992.47.1a–b; Waldman and Evans 1994). The original description of this specimen was carried out without removing the fossil material from the host matrix – a partially metamorphosed limestone, which was resistant to acid preparation. Only relatively superficial mechanical preparation was

undertaken and only the bones revealed on the surface of the blocks were described. Substantial further remains are enclosed within matrix and have not been studied until now.

Here, we provide a re-description and virtual reconstruction of the skull of *Marmoretta* based on synchrotron tomography of NMS G1992.47.1a–b and micro-CT scans of the posterior portions of the mandibular rami from a different specimen, CAMSM X9991 (an incomplete specimen comprising the posterior portion of the right lower jaw; Waldman & Evans 1994). We use the new data from these scans in a phylogenetic analysis using Bayesian inference based on extensive revision of the matrix of Simões et al. (2018). We find that *Marmoretta* is a stem-group lepidosaur, and sister to *Fraxinisaura.*

MATERIAL AND METHODS

NMS G1992.47.1a–b consists of two blocks, one containing the skull and some postcranial material including 14 presacral vertebrae, partial ribs, an interclavicle and clavicles, and partial humerus, radius, ulna, femur and tibia (NMS G1992.47.1a) (Fig. 1), and the second, slightly smaller block, containing more postcranial material including a hand, seven presacral vertebrae with ribs, and the missing portions of humerus, radius, and ulna (split across both blocks) (NMS G1992.47.1b). We used high-resolution computed microtomography (μCT) scanning to make 3D visualisations of the specimen enclosed within the rock. Here we focus on the skull description and phylogenetic implications. Synchrotron computed tomography of the skull block (NMS G1992.47.1a) was carried out at The European Synchrotron Radiation Facility (ESRF) using propagation phase contrast microtomography on the ID17 biomedical beamline. The images generated had an isotropic pixel size of 6.35μm and were produced using a 90 keV monochromatic beam. Overall, 2499 images were produced from the combination of two radiographs with 0.1 second exposure times. The images were reconstructed with PyHST2 (Mirone *et al*. 2014) using the single distance phase retrieval approach (Paganin *et al*. 2002). The final images were then processed post production to change the bit depth from 32 to 16 bits, a weighted average was used for vertical and lateral stitching of the series of acquisition, a ring correction applied (Lyckegaard *et al*. 2011), and finally volume cropping (V Fernandez, pers. comm. 2019). The posterior portions of lower jaws (CAMSM X9991) were scanned at a resolution of 10.4 μm using a Nikon Metrology XT H 225 ST High Resolution CT Scanner at the University of Bristol, School of Earth

Sciences. The specimen was scanned using X-ray settings of 175 kV and 103 µA, with 3141 projections each captured for an exposure time of 0.5 second.

Image volumes were segmented using Mimics Research (http://biomedical.materialise.com/mimics) resulting in 3D models that were exported as .ply files then imported to Blender (http://www.blender.org) for reconstruction and 2D rendering of the figures presented here. Our scan data and 3D models are available on Morphosource [http://www.morphosource.org/projects/000349957~~project url to be entered on acceptance of manuscript~~].

Institutional abbreviations. CAMSM, Sedgwick Museum of Earth Sciences, Cambridge, UK; NHMUK, Natural History Museum, London, UK; NMS, National Museums of Scotland, Edinburgh, UK.

SYSTEMATIC PALAEONTOLOGY

DIAPSIDA Osborn, 1903

LEPIDOSAUROMORPHA Gauthier et al, 1988

Marmoretta, Evans 1991

Type and only species. Marmoretta oxoniensis Evans, 1991

Type specimen. Natural History Museum, London (NHMUK) R12020, anterior portion of right maxilla from the Kirtlington Mammal Bed at the base of the Forest Marble, Old Cement Works Quarry, Kirtlington, Oxfordshire.

Referred specimens. NMS G1992.47.1a–b and CAMSM X9991 and other specimens (Panciroli *et al*. 2020) from Isle of Skye, Scotland, and many isolated additional bones from Kirtlington Old Cement Works, England (Evans 1991, Evans *et al*. 1998), Leigh Delamere, England (Evans & Milner 1994), and Guimarota, Portugal (Evans 1991).

Diagnosis revised from Evans (1991). Small lepidosauromorph; large upper and lower temporal fenestrae; premaxillae paired, each with deep posterolateral maxillary facet; ~~long anterior process of the maxilla,~~ specialized maxillary/premaxillary overlap; small posteroventral process of the jugal; narrow fused frontals; fused parietal forming a broad parietal table, parietal foramen absent, large midline sagittal crest; dorsoventrally wide posterior (squamosal) process of the postorbital that overlaps on to a broad shallow facet on the squamosal; palatine with small teeth that decrease in size medially from a larger row along the medial choana margin to smaller scattered teeth on the ventral surface; pterygoids bear three rows of teeth which radiate anteriorly; long and slender dentary with subpleurodont teeth; coronoid with prominent coronoid process having smooth concave posterior surface which emerges through the lower temporal fenestra.

SKULL DESCRIPTION

The skull is preserved and partially disarticulated in block NMS G-1992.47.1a (Fig. 1). It includes mostly complete fused parietals, fused frontals, left and right prefrontals, almost complete right maxilla, partial right premaxilla, right postfrontal, right postorbital, left and right jugals, right squamosal, right quadrate and quadratojugal, partial left and right ectopterygoids, mostly complete left and right pterygoids, partial left and right palatines, parabasisphenoid, basioccipital, mostly complete right dentary, less complete left dentary, left and right coronoids, broken right prearticular, and a right articular. Post-depositional crushing has resulted in fragmentation and disarticulation of the lower jaws and cranial elements. Waldman and Evans (1994) reconstructed the skull based on the bones observable in the prepared specimen, which did not include new elements revealed by the μCT data, such as the squamosal and the full extent of the parietal crest. We present a new reconstruction of the skull of *Marmoretta* ~~*oxoniensis*~~ using information from NMS G-1992.47.1a and CAMSM X9991 (Fig. 2), including the palatal region, which is poorly preserved.

The dark grey portions of the articulated skull reconstruction are elements that have only been preserved on one side and have been duplicated and mirrored in figures 2A, C, and E. These include the right prefrontal (the right prefrontal is present although less complete than the left - therefore the left prefrontal has been mirrored in this reconstruction), and the entirety of the left mandibular ramus and skull except the jugal and prefrontal. The most

notable of these are the anteroventral process of the postorbital, which is missing, revealing the postorbital facet of the jugal in dorsal view. The anterior process of the maxilla is also missing, leaving the maxillary facet of the premaxilla exposed in lateral and dorsal view. Proposed positions for the nasals and dorsal processes of the premaxilla are also marked by dashed lines in the figure 2B and 2D.

The lack of a preserved squamosal-parietal contact renders the squamosal position provisional and also creates uncertainty with respect to the squamosal-quadrate articulation.

CRANIUM

Premaxilla – A partial right premaxilla is preserved, missing the anterior and posterior portions. Its lateral surface is slightly convex. There are six alveoli, of which only one contains a tooth (Figure 3 E-G). It is likely that at least one more alveolus was present posteriorly, and another anteriorly, giving a minimum of eight marginal teeth in the premaxilla. A mediolaterally deep, 'V'-shaped, maxillary facet is present on the posterolateral surface of the premaxilla. A subnarial ramus extends medially from the anteromedial surface. The ascending anterodorsal process is missing in NMS G-1992.4.7.1a. However, specimens from Kirtlington (NHMUK R12022; [Evans 1991]) show that this process is long and tapers dorsally to separate the external nares across the midline anteriorly, thus dividing the external nares unlike in *Kuehneosaurus* (Evans 2009).

Maxilla – Most of the right maxilla is preserved, but only a partial alveolar shelf of the left maxilla remains. The apex of the dorsal process of the right maxilla is broken, and the facets for the lacrimal and prefrontal are therefore not preserved (Fig.3). The anterior portion of the right maxilla is also incomplete, although the length of the missing section is unknown. The maxilla is elongate and gracile anteroposteriorly, and the dorsal process appears to curve medially, possibly due to deformation. The preserved portion of the anterior process is relatively long, comprising 0.28 of the total anteroposterior length of the maxilla (Fig 3). This is longer than in other stem-group lepidosaurs like *Sophineta*, and most extant squamates, in which the anterior process (AP) is shorter relative to the total maxilla length (ML), (e.g. *Sophineta* AP/ML= 0.13 (Evans & Borsuk-Białynicka 2009); *Iguana*, 0.19; *Japalura*, 0.15; *Hemidactylus*, 0.11; *Tropidophorus*, 0.16; *Cordylus*, 0.21 (Evans, 2008)). Rhynchocephalians

also possess short anterior processes of the maxilla (*Sphenodon* (AP/ML = 0. 13 (Jones 2008)), or even lack them entirely e.g. *Palaeopleurosaurus posidoniae* and *Pleurosaurus goldfussi* (Jones 2008). The long anterior process of *Marmoretta* is similar to that of some squamates such as *Lanthanotus borneensis* (0.38) and varanids (e.g. *Varanus salvator*, 0.31 (Evans, 2008)), but shorter than that of the Triassic stem-lepidosaur, *Fraxinisaura* (AP/ML = 0.51, Schoch & Sues 2018) and the extinct mosasaurians, in which the rostral part of the maxilla can form most of the bone.

A long shallow facet for the jugal is present posterodorsally on the medial surface of the maxilla. Two entrances for the superior alveolar canal are also visible on the dorsal surface of the alveolar shelf; the larger of the two is dorsal to the 16th alveolus, and the smaller is just anterior to this. The palatine facet is a horizontal groove on the alveolar shelf just posterior to the base of the dorsal process. A row of three neurovascular foramina open on the lateral surface of the maxilla, ventral and posterior to the dorsal process, and similar to those seen in *Sophineta* (Evans & Borsuk-Białynicka 2009).

Twenty-three maxillary alveoli are present, 18 of which bear in situ teeth. This is slightly fewer than the estimated total of 25–30 maxillary teeth based on bulk-sample specimens from screenwashing at Kirtlington (Evans 1991). The difference is most likely due to incomplete preservation in NMS G-1992.47.1a. The teeth are conical with a slight apicolingual curvature. Tooth implantation is pleurodont (sensu Bertin *et al.* 2018). There is a substantial difference in height between the labial and lingual walls of the maxilla, with the labial surface of the tooth root attached to the medial side of the labial wall (Fig. 4). This asymmetry of implantation is less evident in the dentary. However, here a basal plate supports the teeth lingually, a condition associated with ‘labial pleurodonty’ (Lessmann 1952, Zaher and Rieppel 1999, Bertin et al. 2018). With the exception of some smaller replacement teeth, the maxillary tooth row is approximately isodont, with tooth heights ranging from ~0.8-0.9 mm.

Prefrontal – The prefrontals are crescentic in lateral view, forming the anterior margin of the orbit. Each prefrontal consists of an anteroposteriorly expanded ventral portion, which has a concave medial surface and convex lateral surface (Fig. 5). From this arises a tapering, rod-like dorsal process that bears a double facet for the frontal on its medial surface, divided by a

narrow longitudinal ridge. Anteroventrally, the prefrontal bifurcates into a short anteromedial process and a longer posterolateral process that curves laterally at an acute angle to form the orbital margin. Specimens from Kirtlington show a broad and shallow facet in between the two prongs – probably for the reception of the lacrimals (Evans 1991), although these are not preserved in NMS G-1992.47.1a.

Jugal – Both the left and right jugals are preserved. These are roughly triangular in lateral view, comprising an anteroposteriorly broad ventral portion that articulates with the maxilla, and a tapering posterodorsal process that contacts the postorbital forming the ventral part of the postorbital bar (Fig. 6). The jugal facet extends further ventrally than the reconstructed ventral tip of the postorbital, and it appears that the ventral process of the postorbital is missing its distal part. The medial surface of the jugal bears a facet anteriorly, which most likely articulated with the ectopterygoid. The anterodorsal surface of the jugal forms the posteroventral rim of the orbit and is mediolaterally thickened compared to its posterior surface. A small posteroventral process is present, entering the anteroventral region of the temporal emargination. Although small, this process is more pronounced than seen in *Sophineta* (Evans & Borsuk-Białynicka 2009), but smaller than that of *Fraxinisaura,* in which the posteroventral process of the jugal is dorsoventrally deep and extends further posteriorly (Schoch & Sues 2018). The absence of the lower temporal bar is a plesiomorphic feature in saurians, as well as being present in some non-saurian neodiapsids such as *Acerosodontosaurus* (Bickelmann *et al*. 2009) and *Lanthanolania* (Modesto & Reisz 2002).

Postorbital – Only the right postorbital is preserved. It comprises three processes (Fig. 7). The ventral process forms the dorsal part of the postorbital bar and bears a facet for the jugal on its posterior surface. The dorsomedial process forms the anterior margin of the upper temporal fenestra and bears a facet for the postfrontal on its anterior surface. The posterior process forms the lateral margin of the upper temporal fenestra and bears a facet for the squamosal on its medial surface. The posterior process is broken and displaced dorsally and has been re-articulated to the anterior region of the postorbital in our reconstructions (Fig. 2A–B). The concave anterior surface of the dorsal and ventral processes forms a large part of the posterior orbital margin (Fig. 7). It is dorsoventrally broad and mediolaterally thin, extending posteriorly to the posterior margin of the temporal region, where it articulates with the lateral surface of the squamosal in an overlapping contact (Fig. 7A). It is rhomboidal with

a curved ventral border. The morphology of the posterior process differs from that seen in Kirtlington specimens (Evans 1991) in which the posterior process is narrower dorsoventrally than seen in NMS G-1992.47.1a. The ventral process of the postorbital as reconstructed by Evans (1991) is also longer and more slender than in NMS G-1992.47.1a. although this apparent difference is probably an artefact caused by the loss of the distal end of the ventral process in the Skye specimen, as indicated by the unoccupied lower half of the postorbital facet on the jugal.

Frontal – The frontals are fused into a median plate with a slightly raised area extending anteroposteriorly along the midline (Fig. 8A). The anteromedial and posterior portions of the bone are damaged and missing. The overall shape of the median frontal is approximately rectangular, transversely broader posteriorly than anteriorly, and narrowest at mid-orbit (around 66% of the posterior transverse width). The ventral margins of the frontal bear distinct cristae cranii that follow the curve of the orbit and are somewhat shallower than in the early rhynchocephalian *Diphydontosaurus* (Whiteside 1986). The dorsal surface of the frontal is anteroposteriorly convex, as is most clearly evident in anterodorsal view (Fig. 8D). The lateral surface is embayed by the dorsal margin of the orbit, suggesting a juvenile or sub-adult ontogenetic stage (see Evans 1991). Well-defined triangular facets for the postfrontals are evident in the posterolateral corners of the bone, tapering anteriorly. Shallow facets for the nasals are present on the preserved anterolateral surface of the frontal, with long prefrontal facets evident along the anterolateral margins.

Postfrontal – Only the right postfrontal is present in NMS G-1992.47.1a (Fig. 9). The overall shape of the bone is triradiate, with a dorsal frontal process, posteromedial parietal process, and ventral postorbital process. The dorsal surface bears a facet for the frontal and the medial surface of the ventral process bears an elongate, triangular facet for the postorbital. This facet extends only for around one-third of the mediolateral width of the postfrontal, leaving a large posteromedial portion that participated in the anterior margin of the upper temporal opening. The posteromedial process is relatively short with a weak parietal facet on its medial surface.

The postfrontal of *Marmoretta* is similar to that of *Sophineta* ((Evans & Borsuk-Białynicka 2009), although in the latter taxon the anteromedial and dorsal processes are somewhat longer.

Parietal – The parietal of *Marmoretta* is a single, fused element. The anterior portion of the parietal is broken on the right side, but well-preserved on the left. This area is not embayed along the midline, and it is likely that a parietal foramen was absent, as noted by Evans (1991). Laterally, the parietal provides the dorsomedial margin of the upper temporal opening. This is best preserved on the left side, where the margin is slightly convex, rather than embayed. The dorsal surface of the parietal bears a prominent, mediolaterally narrow median (sagittal) crest. Either side of the crest, the dorsal surface is transversely convex. Two low, transversely orientated dome-like ridges form distinctive structures on the dorsal surface (Fig. 10). The first dome rises gradually from the fronto-parietal suture, before diminishing sharply to form a transverse fossa approximately half way along the length of the parietal. The second extends posteriorly from this fossa to form a slightly lower dome and shallow fossa. The posterior part of the parietal is inclined posterodorsally from this fossa, forming a short ascending flange at approximately 45°, converging posteriorly to the level of the median crest (Fig. 10). Paired, anteroposteriorly oriented tubercles are present laterally at the base of the short ascending flange (Fig. 10). These tubercles have a hemispherical morphology and merge with the dorsal surface of the parietal anteriorly. The tubercles, and the posterior region of the parietal in general, are broken, but may have continued as lateral processes of the parietal, as in *Huehuecuetzpalli* (Reynoso 1998) and *Dalinghosaurus* (Evans & Wang 2005), or the short ascending flange may have extended posterodorsally, in a similar fashion to that seen in the Permian weigeltisaurid *Coelurosauravus elivensis* (Evans & Haubold 1987; Bulanov & Sennikov 2015).

The large parietal sagittal crest of *Marmoretta* is an unusual feature compared to other early lepidosauromorphs. Some Jurassic and Cretaceous rhynchocephalians (e.g. *Palaeopleurosaurus; Kallimodon; Priosphenodon* (Klein & Scheyer 2017) possess a short crest on a narrow parietal table, with distinctly ventrally orientated lateral flanges (Rieppel 1994). A midline crest on the parietal is also known in several early archosauromorphs (e.g. *Protorosaurus, Macrocnemus, Trilophosaurus* and the rhynchosaurs *Mesosaurus* and *Howesia* (Gottmann-Quesada & Sander 2009; Li, *et al*. 2007; Heckert, *et al*. 2006; Pineiro, *et al*. 2012; Dilkes 1995)). Simões *et al*. (2018 Supp. Info.) suggested that the sagittal crest only occurs in taxa with ventrally directed lateral margins of the parietal, i.e. with a narrow parietal table. *Marmoretta* in an exception in this case in that the skull table is broad and the lateral margins are only moderately ventrolaterally inclined.

Squamosal – The right squamosal is preserved in NMS G-1992.47.1a. and is enclosed in matrix such that it was not described in previous studies (Evans 1991, Waldman and Evans 1994). As preserved, the squamosal is a large, triangular element. The lateral surface curves posteromedially to form a narrow contribution to the occipital region of the cranium (Fig. 11). It is a broadly plate-like bone, lacking clearly defined rami, unlike the tetraradiate squamosal in *Sophineta* or the triradiate squamosals of *Pamelina, Huehuecuetzpalli* and *Megachirella* (Evans 2009; Reynoso 1998; Evans & Borsuk-Białynicka 2009). There is a small posteroventral process, where the bone thickens, which bears a deep, wedge-shaped facet on the posteromedial surface for articulation with the dorsal (cephalic) condyle of the quadrate. The anteroventral process is broken distally, and most likely extended further ventrally, as implied by the presence of a facet on the anterolateral surface of the quadrate dorsal process. The morphology of that facet (Fig. 12) suggests that the ventral process of the squamosal terminated close to or in contact with the dorsal part of the quadratojugal (see Evans 1991). The squamosal lacks an emargination between the postorbital process and the anteroventral process. The lateral surface of the squamosal bears a broad, shallow facet anteroventrally for articulation with the postorbital (Fig. 11). This differs from the tongue and groove articulation of the postorbital/squamosal in *Megachirella* (Simões *et al*. 2018), but is somewhat similar to the same facet in the Lower Jurassic rhynchocephalian *Gephyrosaurus bridensis* (Evans 1980) and the overlapping contact of *Sophineta* where a shallow postorbital facet is also present on the lateral face of the squamosal (Evans & Borsuk-Białynicka 2009). The squamosal tapers dorsally towards its contact with the parietal, although the contact itself is not preserved and cannot be determined. The posterior surface of the squamosal is distinctly concave in lateral view, and this may have supported the tympanic membrane, since a tympanic crest or conch is absent from the quadrate and the retroarticular process is much reduced or absent (Fig, 11).

Quadrate– The right quadrate is preserved in NMS G-1992.47.1a and is similar to the juvenile quadrate of *Marmoretta* (NHMUK R12040) described by Evans (1991) from Kirtlington Quarry. The quadrate consists of a mediolaterally expanded ventral portion that bears the articular condyles for the mandibles, a sheet-like anteromedial process, which extends to contact the quadrate ramus of the pterygoid, and a rod-like dorsal shaft that articulates with the squamosal dorsally via a convex condylar surface. The dorsal shaft also bears a large facet for articulation with the ventral process of the squamosal along its

anterolateral surface. The medial surface of the quadrate shaft which bears a low, horizontal ridge, and may have received the columella of the stapes at the level of the dorsal margin of the quadratojugal.

In ventral view the anteromedial process of the quadrate forms a right angle with the axis of the lateral mandibular condyles. The medial condyle is mediolaterally narrow and anteroposteriorly longer than the lateral condyle, which is mediolaterally wide. The anteromedial process bears a broad, shallow facet for articulation with the pterygoid on its posteromedial surface, and is broken anteriorly (Fig. 12).

The quadrate conch is absent, as noted previously (Evans 1991). The presence of the quadrate conch was considered to be a synapomorphy of Lepidosauriformes (=total-group lepidosaurs excluding kuehneosaurs; equivalent to Lepidosauromorpha here) by Gauthier *et al*. (1988), who considered the conch to be present in *Paliguana*. The lack of a conch in *Sphenodon* represents a secondary loss (Gauthier *et al*. 1988), because the conch is present in basal rhynchocephalians like *Gephyrosaurus and Diphydontosaurus* (Evans 1981; Whiteside 1986). Among early lepidosauromorphs, *Sophineta* also possesses a lateral conch, as does *Megachirella* (Evans & Borsuk-Białynicka 2009; Simões, *et al*. 2018). In general, the quadrate morphology is similar to that of *Sophineta*, although *Sophineta* exhibits a larger depression between the lateral and medial condyles and a straighter dorsal process (Evans & Borsuk-Białynicka 2009).

Quadratojugal — The quadrate of NMS G-1992.47.1a is articulated with a small, lenticular quadratojugal (Fig. 12). The quadratojugal lies ventral to the squamosal facet and may have contacted the squamosal. It articulates with the ventrolateral surface of the quadrate, enclosing a small quadrate-quadratojugal foramen laterally (Fig. 12).

Palatine – Both palatines are both partially preserved in NMS G-1992.47.1a. The thickened maxillary processes are present, but the medial and posterior portions that contact the pterygoids are missing, as are the anterior margins which would contact the vomer. The palatines are thin, dorsally concave plates of bone that have roughly triangular outlines. A field of small teeth is present on the convex palatal surface (Fig. 13). The palatine thickens laterally as it approaches the maxillary process, but the margins of the choana and suborbital

fenestra are not preserved. Palatine teeth are widespread among tetrapods, including stem tetrapods (e.g. *Ichthyostega*), early amniotes (e.g. *Petrolacosaurus*), and many lepidosauromorphs (e.g. *Sophineta*, *Sphenodon*), but have been lost in many squamates (Matsumoto & Evans 2017). In *Marmoretta* the lateral row of palatal teeth is slightly enlarged (Fig. 13), differing from other early lepidosauromorphs except from rhynchocephalians such as *Diphydontosaurus* (Whiteside 1986). The condition in *Marmoretta* is weakly developed in comparison to rhynchocephalians, and we do not consider this to be a directly homologous character. The palatal teeth in NMS G-1992.47.1a are less organised than those in the Kirtlington specimen where distinct tooth rows are apparent. This may be a case of interspecific difference or due to preservation of the Skye specimen, which has resulted in the teeth being disturbed and not preserved in their life position.

Pterygoid – The pterygoids are anteroposteriorly long, each comprising a large, sheet-like palatal process and a narrow quadrate process that extends posterolaterally from the posteromedial part of the palatal process. Both pterygoids are missing their anterior and lateral portions. The broad palatal process has a gently concave ventral surface, and is thickened on the medial edge, which forms the lateral margin of the interpterygoid vacuity (Fig. 14). The palatal surface bears three rows of teeth that radiate anterolaterally from a position just adjacent to the basal articulation. The transverse processes (pterygoid flanges) of both pterygoids are damaged, with only a remnant of the left process remaining. It consists of a roughly triangular extension that thickens along the posterior margin where it joins the main body of the pterygoid lateral to the basal articulation. Overall, the pterygoid is very similar to that of *Fraxinisaura* (Schoch & Sues 2018). There are no teeth present on the transverse process. The quadrate process of the pterygoid curves posterolaterally to meet the medial wing of the quadrate. There is no development of the pit (fossa columellae) on the dorsal surface of the pterygoid quadrate ramus that forms a mobile articulation with the base of the epipterygoid in squamates.

Ectopterygoid – Both ectopterygoids are preserved, although the right bone is more complete than the left, and both are missing their medial portions, including the facet for articulation with the pterygoid. The ectopterygoids are small and comprise an expanded lateral plate for articulation with the maxilla and jugal (Fig, 15) from which a slender stem extends medially

into the palate. The lateral articular surface is flat and dorsomedially deep, with a long, shallow ventral facet for the maxilla and a smaller posterodorsal facet for the jugal. The lateral flange of the ectopterygoid of *Marmoretta* is anteroposteriorly longer than that of *Sophineta* (Evans and Borsuk-Białynicka 2009) and *Diphydontosaurus* (Whiteside 1986). In *Fraxinisaura* the stem is thicker and not smoothly cylindrical (Schoch & Sues 2018).

Parabasisphenoid – The parabasisphenoid is a midline bone that tapers anteriorly, resulting in an approximately triangular outline. It is embayed posteriorly between paired, posterolateral parasphenoid wings. The parasphenoid rostrum (cultriform process) extends anteriorly, but only its base is preserved. The basipterygoid processes extend anteroventrally, the right being broken and the left only partially preserved, (Fig. 16). The posteroventral surface of the parabasisphenoid is concave, and the dorsal surface is also transversely concave and lacks the midline ridge seen in specimens referred to *Marmoretta* from Kirtlington Quarry NHMUK R12055 and NHMUK R12057 (Evans 1991). The internal carotid foramina perforate the ventral surface of the bone and enter the posterolateral part of the hypophysial fossa so that they are not visible in dorsal view. This also differs from the Kirtlington specimens NHMUK R12055 and NHMUK R12057 (Evans 1991) in which the foramina are located anteriorly within the fossa. It also differs from the parabasisphenoid in Fraxinisaura, which bears a patch of denticles on its ventral surface close to the base of the parabasisphenoid (Schoch and Sues 2018).

Basioccipital – The basioccipital forms an ovoid posteroventral occipital condyle (Fig. 17). The ventral surface of the bone bears a low transverse ridge, anterior to the occipital condyle. This becomes more prominent laterally on either side, forming two paired, ventrolaterally-projecting basal tubera. These are relatively large and appear similar to inferred adult specimens referred to *Marmoretta* from Kirtlington (NHMUK R12058 [adult] compared to those of NHMUK R12059 [juvenile] [Evans 1991]). Facets for the exoccipitals are present dorsolaterally on the occipital condyle. The dorsal surface of the basioccipital bears a longitudinal median ridge which spans the posterior two thirds of the bone; on either side of the ridge the bone is concave.

MANDIBLE

Dentary – Both dentaries are incomplete, but the right is the better preserved, although it misses its anterior, posterior, and posteroventral sections. The dentary is long and slender with the medial surface divided into dorsal and ventral parts by the Meckelian groove, which has been narrowed dorsoventrally by post-mortem crushing (Fig. 18). As with the maxillary tooth row, the dentary teeth are implanted in the alveolar shelf, the labial wall of which is higher than the lingual wall, exposing most of the tooth bases lingually. The posterior portion of the right dentary had broken away from the main section of bone and has been repositioned accordingly for the reconstruction. This detached piece contains the posterior-most tooth and facets for the coronoid and surangular on its dorsomedial surface. The Meckelian groove is open medially in the anterior portion of the dentary, similar to NHMUK R12062 (Evans 1991).

Coronoid – Both left and right coronoids are present in NMS G-1992.47.1a and the left is present in CAMSM X9991. They are robust bones, comprising a dorsoventrally broad, sheet-like anteromedial process, a narrow, tapering posterolateral process, and a prominent coronoid process (Fig. 19). The ventral surface of the coronoid bears a groove-like horizontal facet for articulation with the dorsal surface of the dentary. The anteromedial process extends ventral to this, covering a portion of the medial surface of the dentary. The lateral surface of the anteromedial flange bears a small posterior facet for the prearticular. The coronoid process curves medially to produce a smooth concave posterior surface which serves as an attachment site for the mandibular adductor (Evans 1991).

Splenial – The splenial is not preserved in NMS G-1992.47.1a. However, it is present in articulation with the other bones of the posterior part of the mandible in CAMSM X9991. The splenial in CAMSM X9991 is incomplete, comprising only the posteroventral and posterodorsal parts of the bone, which are broken and appear as separate fragments. These articulate with the dentary, coronoid and prearticular.

Prearticular – The right prearticular is present in both associated specimens of *Marmoretta*. In NMS G1992.47.1a it is broken in half dorsoventrally and is missing the anterior and posterior ends. In CAMSM X9991 the prearticular is preserved in articulation with the rest of

the lower jaw bones, aiding the analysis of NMS G1992.47.1a (Fig. 19). On the medial surface of the bone there is a shallow impression bordered dorsally by a low ridge that runs anterodorsally-posteroventrally, ending about three quarters of the way along the bone. This marks the dorsal extent of the splenial facet. On the lateral surface there is a long v-shaped facet for the dentary positioned anteriorly on the thickened dorsal margin. Posteriorly the prearticular tapers to a point at which the ventral surface is contacted by the angular, and the dorsal surface by the articular.

Surangular – The right surangular is present in both NMS G1992.47.1a and CAMSM X9991, although it is more complete in the latter. The bone is long, extending from the posteroventral surface of the dentary, adjacent to about the 6th from last tooth, to the ventral surface of the articular. On the anterolateral surface there is a long, broad and shallow facet for the posterior region of the dentary and, just ventral to the tip of the dentary, there is an anterior surangular foramen. Posteriorly the surangular expands into a broad cup-like facet for the articular. Ventrally the surangular contacts the prearticular anteroventrally and the angular posteroventrally (Figs. 19 B and C).

Angular – The angular is not preserved in NMS G1992.47.1a, but the right bone is evident in CAMSM X9991. It is a small slender element that tapers at its anterior and posterior ends. The angular is positioned on the ventral surface of the lower jaw and contacts the surangular dorsolaterally, the prearticular and the articular dorsomedially (anterior – posterior), and the splenial ventrally.

Articular – The right articular is present in both associated specimens. It is a robust bone that makes up the posterior end of the lower jaw, with its dorsal surface articulating with the condyles of the quadrate. The ventral surface of the articular has a narrow but relatively deep medial facet for the prearticular. The medial surface of the bone continues dorsally from this facet and is mostly flat, expanding slightly at the dorsal surface. On the lateral side the articular is broad posteromedially and the ventrolateral surface narrows ~~on the diagonal~~medially to form the lateral surface of the prearticular facet. The broad posteromedial portion of the bone is sheathed from below by the large surangular facet. Dorsally the articular slopes anteroposteriorly at an angle of ~45°. The dorsal surface is

divided by a central groove that is bordered by a tall projection medially, and a shorter, broader projection on the lateral side.

There is no development of a retroarticular process.

DISCUSSION

Our high-resolution synchrotron tomography of referred specimens of *Marmoretta ~~oxoniensis~~* (NMS G-1992.47.1, CAMSM X9991) provides important new anatomical data. In particular it has clarified our understanding of the suspensorium and posterior region of the mandible, demonstrated the extent of the parietal sagittal crest and the pleurodont nature of the marginal tooth implantation. Our reconstruction of the skull of *Marmoretta* retains much of the general form of previous studies (Evans 1991, Waldman and Evans 1994). However, the dorsoventral height of the postorbital region of the cranium and the posterior portion of the mandible suggest a distinctive, anteriorly tapering skull-shape, augmented by the prominent sagittal crest.

The sagittal crest of *Marmoretta* differs from that of other reptiles in that it is combined with a transversely broad parietal table. The crest provides an attachment site for the external adductor muscle, which descends to attach to the medial surface of the coronoid eminence in the mandible. The coronoid eminence of *Marmoretta* bears a large concavity on the posteromedial surface for this adductor attachment, suggesting a strong closing force (King 1996). Although comparatively powerful bite-force is postulated in small (>2.5cm skull length) early Mesozoic diapsids, it is correlated with transversely narrow parietal tables and broad upper temporal openings in relation to the transverse width of the postorbital region (Pritchard *et al.* 2018). *Marmoretta* does not possess either of these features, although the adductor musculature in *Marmoretta* would have benefitted from extended dorsoventral length and may represent an ecomorphologically diverse approach to substantial bite-force in small diapsids.

The arrangement of the palatal teeth in NMS G-1992.47.1a differs from that recorded by Evans (1991) based on specimens from Kirtlington Old Cement Quarry (NHMUK R12045, R12046, R12047). NMS G-1992.47.1a possesses lateral palatine teeth that are slightly enlarged and are not positioned into distinct rows, unlike in the Kirtlington

specimens. Also, the pterygoid of NMS G-1992.47.1a bears three tooth rows as opposed to the two described in the Kirtlington specimens (Evans, 1991; NHMUK R12052, R12054). However, this is likely due to the more complete preservation of the pterygoids in NMS-G 1992.47.1a compared to NHMUK R12052 and R12054.

Palatal teeth are considered an ancestral condition in amniotes, and appear in one form or another in most major clades although there is a general pattern of reduction in many lineages (Matsumoto & Evans 2017). Nevertheless, the morphology and inferred function of palatal teeth varies among taxa. The longitudinal rows of palatal teeth seen in *Marmoretta* suggest that they may have assisted with moving food towards the back of the mouth (Matsumoto & Evans 2015). In many extant lepidosaurs this function is carried out by a muscular tongue in conjunction with varying amounts of palatal dentition (Matsumoto & Evans 2017). The presence of anterior palatal teeth in *Marmoretta* (palatine and pterygoid, possibly vomer although this is unknown) and lack of posterior palatal teeth (parabasisphenoid and transverse process) suggest their main function was intraoral transport and that they were likely accompanied by a mobile tongue.

There are a few other differences between this specimen NMS G-1992.47.1a and the Kirtlington specimens NHMUK R12037 (a juvenile postorbital) and NHMUK R12055 and NHMUK R12057 (parabasisphenoids) described by Evans (1991). These include the shape of the posterior process of the postorbital which is dorsoventrally taller in NMS G-1992.47, and the positioning of the internal carotid foramina within the hypophysial fossa which are further posterior in this specimen. These may be examples of ontogenetic or intraspecific variation, or indicate that the assemblage from Kirtlington includes a different species to the specimens described here.

Phylogenetic analysis. Earlier studies have resulted in two hypotheses on the affinities of *Marmoretta*. Evans (1991) interpreted *Marmoretta* as a non-lepidosaurian lepidosauromorph, outside of the crown-group split between rhynchocephalians and squamates, based on material from Kirtlington, Oxfordshire. New data from specimens collected from the Isle of Skye (Waldman and Evans 1994) and subsequent analyses (Evans and Borsuk-Białynicka 2009; Evans 2009, Evans & Jones 2010; Jones *et al.* 2013) have generally re-iterated this view. The recent phylogenetic analysis of Schoch and Sues (2018) also recovered *Marmoretta* as a stem-group lepidosaur, as sister to the Middle Triassic *Fraxinisaura rozynekae*. In contrast to this hypothesis, Simões *et al.* (2018) recovered *Marmoretta*, along with *Megachirella* from the Middle Triassic of Italy, as a stem-group squamates, within Lepidosauria, using both parsimony analysis and Bayesian inference.

To evaluate the phylogenetic position of *Marmoretta* based on the new data, we used a modified version of the 347 characters in the morphological dataset of Simões *et al.* (2018). We added 32 new characters and removed two, making a total of 377 characters. These changes are based on an extensive review of their dataset and published comparative literature and our modifications are described more completely in the Supplementary Data. Of the 32 new characters, two replaced existing characters and describe distinctive aspects of similarity among the squamosals of squamates that are absent outside the squamate crown-group (e.g. Evans 2008). Overall, our additions mostly reflect comparative observations that were framed by older literature, but were not included in the original character list of Simões *et al*. (2018). These observations document variation among early crown-group reptiles and especially among early lepidosauromorphs, encoding character state variation that has been influential for existing phylogenetic hypotheses (e.g. Camp 1923; Parrington 1958). We also revised the scores of several taxa, focusing on those that have previously been considered as early lepidosauromorphs (e.g. *Megachirella, Sophineta, Palaeagama, Gephyrosaurus and Diphydontosaurus*) or potentially closely related taxa ,*(e.g. Kuehneosaurus* and *Pamelina*). We omitted some taxonomic units, and added others such as *Fraxinisaura*. A list of these modifications together with explanatory notes is included in Supplementary Data.

We performed a non-time calibrated Bayesian analysis of the resulting data using the Mkv model with using MrBayes v.3.2.5. as described in Supplementary Data 1, using a maximum clade credibility tree (MCC) to summarize the results of this analysis (Fig. 20).

The MCC tree recovers *Marmoretta* as a stem-group lepidosaur (i.e. a non-lepidosaurian lepidosauromorph), in agreement with some previous studies (Evans 1991, Jones *et al.* 2013). We also find *Marmoretta* as a sister taxon of the Middle Triassic *Fraxinisaura*, within an early diverging and geologically long-lived clade of non-lepidosaurian lepidosauromorphs. This is consistent with the phylogenetic hypotheses posited by Schoch and Sues (2018), who noted the striking similarity of the maxillae of *Marmoretta* and *Fraxinisaura*, which both possess a low, triangular facial process and elongate anterior process. We find this group (*Marmoretta* + *Fraxinisaura*) is supported by three unambiguous synapomorphies (the absence of the premaxillary process of the maxilla c.20.1, the absence of a parietal foramen c.73.1 and the absence of an infraorbital foramen on the palatine c.101.1) The clade comprising *Marmoretta* + *Fraxinisaura* also possesses several lepidosauromorph synapomorphies, including a reduced lacrimal (under deltran c.360.1), pleurodont implantation of maxillary dentition (under acctran c.213.0), a quadratojugal foramen (unambiguous c.42.1) and an 'hour-glass' shaped frontal (under acctran c.354.1).

Our phylogenetic findings therefore differ from those of Simões *et al.* (2018), who recovered *Marmoretta* as a stem-group squamate, nested within Lepidosauria (i.e. as a member of the crown-group). Consistent with our recovery of *Marmoretta* in the stem-group, we observe various features that are present in crown-group lepidosaurs, but are absent in *Marmoretta*. These features include subolfactory processes of the frontals (unambiguous c.69.1) and the lateral conch of the quadrate (under deltran c.121.1). The absence of a lateral conch of the quadrate in *Marmoretta* may be plesiomorphic for lepidosauromorphs, with the lateral conch probably appearing closer to the divergence of the crown-group in more derived stem-lepidosaurs. The quadrate conch is present in squamates and early rhynchocephalians (Evans 1980, Whiteside 1986, Simões *et al.* 2018) and, probably, convergently in kuehneosaurs (Evans 2009). Unfortunately, the condition in the quadrate is unknown in *Fraxinisaura* (Schoch and Sues 2018). Further, *Marmoretta* possesses several features that are not found in squamates (e.g. quadratojugal present c.38.0, absence of a notch for the squamosal on the cephalic head of the quadrate c.123.0, the ventral exposure of the entry foramen for the internal carotid artery in the basisphenoid c.124.1), or in rhynchocephalians (e.g. the absence of frontal tabs on the parietal, c.78.1, the presence of a splenial c.176.1, the absence of a notochordal canal in adults, c.229.1).

Megachirella from the Middle Triassic of Italy, like *Marmoretta*, was originally reported as a non-lepidosaurian lepidosauromorph (Renesto & Posenato, 2003) but subsequently recovered as a stem-squamate inside of the lepidosaurian crown-group by Simões et al. (2018). Our MCC tree, recovers *Megachirella* as a stem-squamate, in accordance with Simões *et al* (2018). *Megachirella* shares several key features with lepidosaurs e.g. a lateral quadrate conch (c.121.1) and with squamates e.g. the loss of the anteroventral process of the squamosal (c.50), although both of these character states are also found in kuehneosaurs, which were not recovered as lepidosauromorphs in our analysis. We also recover *Sophineta*, which generally has been described as a non-lepidosaurian lepidosauromorph (Evans and Borsuk-Białynicka 2009, Jones *et al.* 2013), as a basal squamate (in the MCC tree). However, it is notable that support for both *Megachirella* and *Sophineta* as squamates is poor in the MCC tree (posterior probability = 0.36 and 0.08 respectively), and both taxa are found in a trichotomy with squamates and rhynchocephalians in the 50% majority rule tree from our posterior sample (see Supplementary Data).

Our analysis also highlights substantial uncertainties regarding to the phylogenetic positions of other taxa traditionally interpreted as basal lepidosauromorphs, with *Paliguana* recovered outside Lepidosauromorpha in both tree topologies (Fig. 20 and Supplementary Data). The anatomy, affinities and evolutionary implications of this taxon require further investigation.

CONCLUSIONS

New anatomical data on the skull of *Marmoretta oxoniensis* from the Middle Jurassic of the UK and Late Jurassic of Portugal has significantly added to our knowledge of this taxon. Based on these new data, our phylogenetic analysis recovers *Marmoretta* as a member of the lepidosaurian stem lineage, and a sister taxon to the Middle Triassic *Fraxinisaura.* This differs from the hypothesis proposed by Simões *et al*. (2018) who recovered *Marmoretta* as a squamate, within the lepidosaurian crown-group. As a Middle Jurassic taxon, *Marmoretta* remains significantly younger than other stem-group lepidosaurs, including its closest known relative *Fraxinisaura*. Both taxa are members of a clade that co-existed with the crown-group for at least 80 million years, and likely became extinct before the end of the Mesozoic,

leaving rhynchocephalians and squamates as the sole representatives of the lepidosaurian line.

ACKNOWLEDGEMENTS

Our thanks to Dr Michael Waldman who collected NMS G1992.47.1a–b, to the National Museums Scotland for access to the specimen and permission to partially prepare it, and to the John Muir Trust and Scottish Natural Heritage who are responsible for permitting fieldwork on the protected fossil localities on the Elgol Coast Site of Special Scientific Interest. Thanks to the Sedgwick Museum Cambridge for the loan of the CAMSM X9991 and permission to scan it, and to the scanning unit at the University of Bristol. We acknowledge the European Synchrotron Radiation Facility for provision of synchrotron radiation facilities (proposal LS 2546), and we would like to thank Vincent Fernandez for assistance in using beamline ID17 to scan NMS G1992.47.1a–b.~~We thank V. Fernandez, who conducted synchrotron tomography of NMS G1992.47.1a–b~~.

AUTHOR CONTRIBUTION

Elizabeth Griffiths carried out investigation and formal analysis of the μCT data and visualisation of 3D models into manuscript figures, as well as writing of the original manuscript draft. David Ford carried out formal analysis of the phylogenetic data and wrote the phylogenetic discussion in the manuscript as well as the supplementary data. Roger Benson conceptualised, managed and supervised the project, and led review and editing of the manuscript, assisted by all other authors. Susan Evans assisted in review and editing of the manuscript and validation of the character matrix scoring.

REFERENCES

BERTIN, T.J., THIVICHON-PRINCE, B., LEBLANC, A.R., CALDWELL, M.W. & VIRIOT, L., 2018. Current perspectives on tooth implantation, attachment, and replacement in Amniota. *Frontiers in Physiology*, **9**, 1630.

642 BICKELMANN, C., MULLER, J., REISZ, R. R. 2009. The enigmatic diapsid
643 *Acerosodontosaurus piveteaui* (Reptilia: Neodiapsida) from the Upper Permian of Madagascar
644 and the paraphyly of "younginiform" reptiles. *Canadian Journal of Earth Sciences,* **46** (9),
645 651–661.

646 BULANOV, V. V. & SENNIKOV, A. G. 2015. Substantiation of validity of the Late
647 Permian genus *Weigeltisaurus* Kuhn, 1939 (Reptilia, Weigeltisauridae). *Paleontological*
648 *Journal*, **49** (10), 1101–1111.

649 CAMP, C. L. 1923. Classification of the lizards. *Bulletin American Museum of Natural*
650 *History,* **48**, 289-481.

651 CARROLL, R. L. 1975. Permo−Triassic "lizards" from the Karroo. *Palaeontologia africana,*
652 **18**, 71-87.

653 DILKES, D. W. 1995. The rhynchosaur *Howesia browni* from the lower Triassic of South
654 Africa. *Palaeontology*, **38**, 665-685.

655 EVANS, S. E. 1980. The skull of a new eosuchian reptile from the Lower Jurassic of South
656 Wales. *Zoological Journal of the Linnean Society*, **70**, 203–264.

657 EVANS, S. E. 1981. The postcranial skeleton of the Lower Jurassic eosuchian
658 *Gephyrosaurus bridensis*. *Zoological Journal of the Linnean Society*, **73** (1), 81–116.

659 EVANS, S. E. 1991. A new lizard-like reptile (Diapsida: Lepidosauromorpha) from the
660 Middle Jurassic of England. *Zoological Journal of the Linnean Society*, **103**, 391-412.

661 EVANS, S.E. 2003. At the feet of the dinosaurs: the early history and radiation of lizards.
662 *Cambridge Philosophical Society: Biological Reviews*. **78** (4), 513-551.

663 EVANS, S.E. 2008. The skull of lizards and Tuatara. *In:* C. GANS, AS. GAUNT, K.
664 ADLER, eds. *Biology of the Reptilia.* Vol. 20: *The skull of Lepidosauria*, Society for the
665 Study of Amphibians and Reptiles, Ithaca, New York, 1-347.

666 EVANS, S. E. 2009. An early kuehneosaurid reptile (Reptilia: Diapsida) from the Early
667 Triassic of Poland. *Palaeontologia Polonica*, **65**, 145-178.

EVANS, S. E. & BORSUK-BIAŁYNICKA, M. 2009. A small lepidosauromorph reptile from the Early Triassic of Poland. *Palaeontologia Polonica*, **65**, 179-202.

EVANS, S. E. & HAUBOLD, H. 1987. A review of the Upper Permian genera *Coelurosauravus, Weigeltisaurus* and *Gracilisaurus* (Reptilia: Diapsida). *Zoological Journal of the Linnean Society,* **90**, 275-303.

EVANS, S. E. & JONES, M. E. H. 2010. The origin, early history and diversification of lepidosauromorph reptiles. *In*: S. BANDYOPADHYAY, ed. *New Aspects of Mesozoic Biodiversity*. Springer-Verlag, Berlin Heidelberg, 27-44.

EVANS, S.E. and MILNER, A.R. 1994. Middle Jurassic microvertebrate assemblages from the British Isles. *In:* FRASER, N. C. and SUES, H.-D. (eds). *In the shadow of the dinosaurs: Early Mesozoic tetrapods*. Cambridge University Press, 303-321.

EVANS, S. & WANG, Y. 2005. The Early Cretaceous lizard *Dalinghosaurus* from China. *Palaeontologica Polonica*, **50** (4), 725–742.

EZCURRA, M. D., SCHEYER, T. M. & BUTLER, R. J. 2014. The origin and early evolution of Sauria: reassessing the Permian saurian fossil record and the timing of the crocodile-lizard divergence. *PLoS ONE*, **9** (2), 1-36.

GAUTHIER, J., ESTES, R. & DE QUEIROZ, K. 1988. A phylogenetic analysis of Lepidosauromorpha. *In*: R. ESTES & G. PREGILL, eds. *Phylogenetic Relationships of the Lizard Families*. Stanford University Press, Stanford, 15-98.

GOTTMANN-QUESADA, A. & SANDER, P. M. 2009. A redescription of the early archosauromorph *Protorosaurus speneri* MEYER, 1832, and its phylogenetic relationships. *Palaeontographica,* Abteilung. A, **287**, 123-220.

GRADSTEIN, F. M., OGG, J. G., SCHMITZ, M. D., OGG, G. M. 2012. *Geologic Time Scale 2012*. Elsevier, Oxford, 1176.

HECKERT, A. B LUCAS, S. G., RINEHART, L. F., SPIELMANN, J. A., HUNT, A. P., KAHLE, R. 2006. Revision of the archosauromorph reptile *Trilophosaurus*, with a description of the first skull of *Trilophosaurus jacobsi*, from the Upper Triassic Chinle Group, West Texas, USA. *Palaeontology*, **49**, 621-640.

JONES, M. E. H. 2008. Skull shape and feeding strategy in *Sphenodon* and other Rhynchocephalia (Diapsida: Lepidosauria). *Journal of Morphology*, **269**, 945-966.

JONES, M.E., ANDERSON, C.L., HIPSLEY, C.A. *et al*. 2013. Integration of molecules and new fossils supports a Triassic origin for Lepidosauria (lizards, snakes, and tuatara). *BioMed Central Evolutionary Biology*, **13**:208, 1-21.

KING, G. 1996. *Reptiles and Herbivory*. First ed. Chapman & Hall, London. 176.

KLEIN, N. & SCHEYER, T. M. 2017. Microanatomy and life history in *Palaeopleurosaurus* (Rhynchocephalia: Pleurosauridae) from the Early Jurassic of Germany. *The Science of Nature*, **104**(4).

LESSMANN, M. 1952. Zur labialen Pleurodontie an Lacertilier-Gebissen. *Anatomischer Anzeiger,* **99**, 35–67.

LI, C., ZHAO, L. & WANG, L. 2007. A new species of *Macrocnemus* (Reptilia: Protorosauria) from the Middle Triassic of southwestern China and its palaeogeographical implication. *Science in China Series D: Earth Sciences*, **50** (11), 1601-1605.

LYCKEGAARD, A., JOHNSON, G. & TAFFOREAU, P. 2011. Correction of ring artifacts in X-ray tomographic images. *International Journal of Tomography & Statistics*, **18**, 1-9.

MATSUMOTO, R. & EVANS, S. E. 2015. Morphology and function of the palatal dentition in Choristodera. *Journal of Anatomy*, **228** (3), 414-429.

MATSUMOTO, R. & EVANS, S. E. 2017. The palatal dentition of tetrapods and its functional significance. *Journal of Anatomy*, **230**, 47-65.

MIRONE, A., BRUN, E., GOUILLART, E., TAFFOREAU, P., KIEFFER, J. 2014. The PyHST2 hybrid distributed code for high speed tomographic reconstruction with iterative reconstruction and a priori knowledge capabilities. *Nuclear Instruments and Methods in Physics Research Section B: Beam Interactions with Materials and Atoms*, **324**, 41-48.

MODESTO, S. P. & REISZ, R. R. 2002. An enigmatic new diapsid reptile from the Upper Permian of eastern Europe. *Journal of Vertebrate Paleontology,* **22** (4), 851-855.

OSBORN, H.F. 1903. The reptilian subclasses Diapsida and Synapsida and the early history of the Diaptosauria. *Memoirs of the American Museum of Natural History*. **1**, pt. 8.

PAGANIN, D., MAYO, S., GUREYEV, T. E., MILLER, P. R., WILKINS, S. W. 2002. Simultaneous phase and amplitude extraction from a single defocused image of a homogeneous object. *Journal of Microscopy,* **206** (1), 33-40.

PANCIROLI, E., BENSON, R. B. J., WALSH, S., BUTLER, R. J., CASTRO, T. A., JONES, M. E. H., and EVANS. S. E. 2020. Diverse vertebrate assemblage of the Kilmaluag Formation (Bathonian, Middle Jurassic) of Skye, *Scotland. Earth and Environmental Science Transactions of the Royal Society of Edinburgh*, 1–22.

PARRINGTON, F. R. 1958. The problem of the classification of reptiles. *Zoological Journal of the Linnean Society*, **44**, 99-115.

PINEIRO, G., FERIGOLO, J., RAMOS, A. & LAURIN, M. 2012. Cranial morphology of the Early Permian mesosaurid *Mesosaurus tenuidens* and the evolution of the lower temporal fenestration reassessed. *Comptes Rendus Palevol*, **11**, 379-391.

PRITCHARD, A.C., GAUTHIER, J.A., HANSON, M. ET AL. 2018. A tiny Triassic saurian from Connecticut and the early evolution of the diapsid feeding apparatus. *Nature Communications,* **9**, 1213.

RENESTO, S. & BERNARDI, M. Redescription and phylogenetic relationships of *Megachirella wachtleri* Renesto et Posenato, 2003 (Reptilia, Diapsida). *Paläontol Z* **88**, 197–210.

RENESTO, S. & POSENATO, R. A new lepidosauromorph reptile from the Middle Triassic of the Dolomites (Northern Italy). *Rivista Italiana di Paleontologia e* Stratigrafia. **109**, 463–474.

REYNOSO, V.-H. 1998. *Huehuecuetzpalli mixtecus* gen. et sp. nov: a basal squamate (Reptilia) from the Early Cretaceous of Tepexi de Rodríguez, Central México. *Philosophical Transactions of the Royal Society London B*, **353** (1367), 477-500.

RIEPPEL, O. 1994. Chapter 2 - Lepidosauromorpha: an overview. *In*: N. C. FRASER & H. -D. SUES, eds. *In the Shadow of the Dinosaurs*. Cambridge University Press, Cambridge, 23-37.

SCHOCH, R. R. & SUES, H.-D. 2018. A new lepidosauromorph reptile from the Middle Triassic (Ladinian) of Germany and its phylogenetic relationships. *Journal of Vertebrate Palaeontology*, **38** (2), 1-14.

SIMÕES, T. R. CALDWELL, M. W., TALANDA, M., BERNADI, M., PALCI, A., VERNYGORA, O., BERNARDINI, F., MANCINI, L., NYDAM, R. L. 2018. The origin of squamates revealed by a Middle Triassic lizard from the Italian Alps. *Nature*, **557**, 706-720.

WALDMAN, M., EVANS S.E. 1994, Lepidosauromorph reptiles from the Middle Jurassic of Skye. *Zoological Journal of the Linnean Society*, **112**, 135-150.

WHITESIDE, D. I. 1986. The head skeleton of the Rhaetian sphenodontid *Diphydontosaurus avonis* gen. et sp. Nov. and the modernising of a living fossil. *Proceedings and Philosophical Transactions of the Royal Society, Series B*, **312**, 379-430.

ZAHER, H., & RIEPPEL, O. 1999. Tooth implantation and replacement in squamates, with special reference to mosasaur lizards and snakes. *American Museum Noviates.* **3271**, 1–19.

FIG. 1. A, NMS G-1992.47.1a. B, renderings of tomographic data showing transparent blocks of specimen NMS G-1992.47.1a&b with segmented bones shown inside the semi-transparent blocks, C, segmented bones in preserved position shown enlarged. Scale bar = 10mm.

FIG. 2. Digital skull reconstruction of *Marmoretta oxoniensis*, using information from NMS G-1992.47.1a and CAMSM X9991, in A–B, lateral, C–D, dorsal and E–F ventral views. Grey shading is used in line drawings (B,D,F) to provide information on depth. Abbreviations: an = angular; ar = articular; cor = coronoid; d = dentary; ect = ectopterygoid; fr = frontal; j = jugal; mx = maxilla; pa = palatine; par = parietal; pbp = parabasisphenoid; pmx = premaxilla; po.f = postfrontal; po.or = postorbital; pr.a = prearticular; prf = prefrontal; ptg = pterygoid; qu

= quadrate; s.a = surangular; sq = squamosal. Dashed lines indicate broken/restored regions of the cranium. Scale bar = 1mm.

FIG. 3. *Marmoretta*, Skye, specimen NMS G-1992.47.1a. Right maxilla in A, lateral, B, dorsal, C, medial, and D, ventral views. Right premaxilla in E, lateral, F, dorsal, and G, ventral views. Abbreviations: alv.b = alveolar border; d.p = dorsal process; j.f = jugal facet; m.f = maxilla facet; ne.f = neurovascular foramina pa.f = palatine facet; sac.e = superior alveolar canal entrance; sn.r = subnarial ramus. Dashed lines indicate broken/restored regions of the bone. Scale bar =1mm.

Fig. 4. *Marmoretta*, Skye, specimen NMS G-1992.47.1a. Cross section (A) and interpretive drawing (B) of tooth implantation in the maxilla and dentary. Abbreviations: bp = basal plate; d(lab) = dentary labial wall; d(lin) = dentary lingual wall; dt = mature dentary tooth; f = nutrient foramina; m(lab) = maxilla labial wall; m(lin) = maxilla lingual wall; mt = emerging maxillary tooth.

FIG. 5. *Marmoretta*, Skye, specimen NMS G-1992.47.1a. Right prefrontal in A, dorsal, B, ventral, and C, lateral views. Abbreviations: fr.f = frontal facet; l.f = lacrimal facet; mx.f = maxillary facet; orb.b = orbital border; p.p = palatine process. Scale bar = 1mm.

FIG. 6. *Marmoretta*, Skye, specimen NMS G-1992.47.1a. Right jugal in A, lateral, B, dorsomedial oblique and C, medial views. Abbreviations: ect.f = ectopterygoid facet; mx.f = maxillary facet; po.f = postorbital facet; pv.p = posteroventral process. Scale bar = 1mm.

FIG. 7. *Marmoretta*, Skye, specimen NMS G-1992.47.1a. Right postorbital in A, lateral, B, anterolateral oblique and C, medial views. Abbreviations: j.f = jugal facet; orb.b = orbital border; pf.f = postfrontal facet; sq.f = squamosal facet. Dashed lines indicate broken/restored regions of the bone. Scale bar = 1mm.

FIG. 8. *Marmoretta*, Skye, specimen NMS G-1992.47.1a. Frontal in A, dorsal, B, oblique right posterolateral, C, ventral and D, anterodorsal views. Dashed lines show estimated outlines of original bone before breakage, and are used to indicate broken regions. Dotted line

in C estimates the ventral portion of the bone. Abbreviations: c.c = cristae cranii; n.f = nasal facet; pf.f = postfrontal facet; prf.f = prefrontal facet. Scale bar = 1mm.

FIG. 9. *Marmoretta*, Skye, specimen NMS G-1992.47.1a. Right postfrontal in A, lateral, B, medial and C, ventromedial views. Abbreviations: fr.f = frontal facet; orb.b = orbital border; par.f = parietal facet; po.f = postorbital facet. Scale bar = 1mm.

FIG. 10. *Marmoretta*, Skye, specimen NMS G-1992.47.1a. Parietal in A, dorsal, and B, right lateral views. Abbreviations: acs.f = ascending flange ; ml.c = midline crest; tu = tubercle. Dashed lines are to highlight the depressions between the domes as well as broken/estimated bone outlines. Scale bar = 1mm.

FIG. 11. *Marmoretta*, Skye, specimen NMS G-1992.47.1a. Right squamosal in A, lateral, B, medial and C, posterior views. Abbreviations: po.f = postorbital facet; qu.f = quadrate facet. Scale bar = 1mm.

FIG. 12. *Marmoretta*, Skye, specimen NMS G-1992.47.1a. Right quadrate and quadratojugal in A, lateral, B, medial, C, ventral, D, anterior, E, posterior and F, dorsal views. Abbreviations: pt.f = pterygoid facet; quj = quadratojugal; quj.f = quadratojugal foramen; sq.f = squamosal facet. Dashed lines indicate broken/restored regions of the bone. Scale bar = 1mm.

FIG. 13. *Marmoretta*, Skye, specimen NMS G-1992.47.1a. Left and right palatine in A, ventral view and B, dorsal view. Abbreviations: max. ram = maxillary ramus; subo.f.m = suborbital fenestra margin; t = teeth. Scale bar = 1mm.

FIG. 14. *Marmoretta*, Skye, specimen NMS G-1992.47.1a. Left and right pterygoids in A, ventral and B, dorsal views. Abbreviations: b.a = basal articulation; md.f = midline facet; pa.f = palatine facet; pp = palatal plate ; qp = quadrate process; tp = transverse process. Dashed lines indicate broken/restored regions of the bone. Scale bar = 1mm.

FIG. 15. *Marmoretta*, Skye, specimen NMS G-1992.47.1a Right maxilla, jugal and ectopterygoid in medial view A without ectopterygoid showing facet on jugal, B with ectopterygoid and C dorsal view. Abbreviations: ect.f = ectopterygoid facet; ect = ectopterygoid; j = jugal; mx = maxilla. Scale bar = 1mm.

FIG. 16. *Marmoretta*, Skye, specimen NMS G-1992.47.1a. Parabasisphenoid in A, dorsal, B, ventral and C, posteroventral views. Abbreviations: bpt.p = basipterygoid processes; cv = cristae ventrolaterales; hf = hypophysial fossa; ica = internal carotid foramen; ppw = posterior parasphenoid wing; psr = parasphenoid rostrum. Dashed lines indicate broken/restored regions of the bone. Scale bar = 1mm.

FIG. 17. *Marmoretta*, Skye, specimen NMS G-1992.47.1a. Basioccipital in A, dorsal, B, ventral and C, posterior views. Abbreviations: bt = basal tubera; eo.f = exoccipital facet; oc = occipital condyle. Scale bar = 1mm.

FIG. 18. *Marmoretta*, Skye, specimen NMS G-1992.47.1a. Right dentary in A, lateral, B, dorsal, C, medial, and D, ventral views. Abbreviations: alv.s = alveolar shelf; cor.f = coronoid facet ; M.f = Meckelian fossa; t = teeth. Scale bar = 1mm.

FIG. 19. *Marmoretta oxoniensis*, referred specimen CAMSM X9991. Right lower jaw approximately as preserved, with slight reconstruction to move the prearticular, splenial and angular into place. A dorsal, B, lateral, C, ventral and D, medial views. Abbreviations: an = angular; ar = articular; c = coronoid; d = dentary; pr.a = prearticular; s.a = surangular; sp = splenial. Scale bar = 1mm.

FIG. 20. Maximum clade credibility tree recovered from Bayesian analysis using non-time calibrated Mkv model. Figures adjacent to nodes are the posterior probability value of the node.

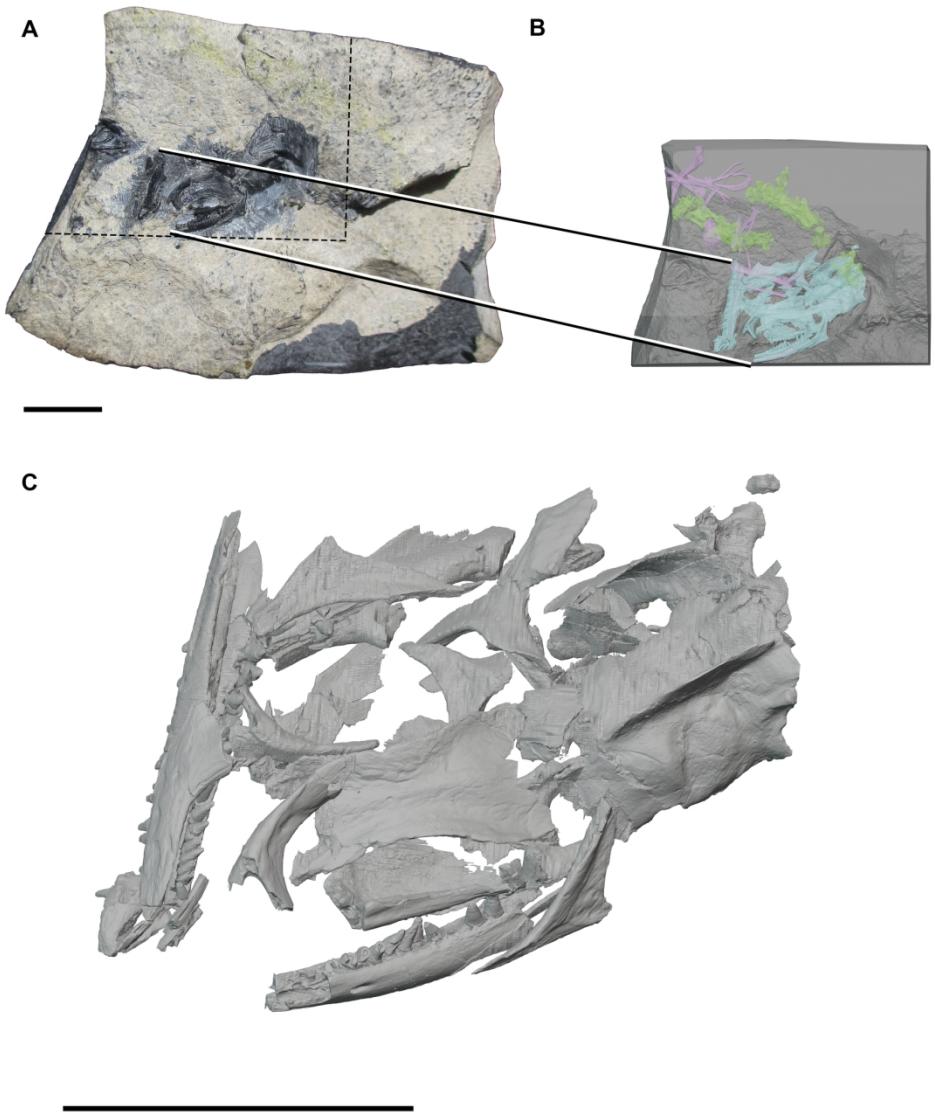

FIG. 1. A, NMS G 1992.47.1a. B, renderings of tomographic data showing transparent blocks of specimen NMS G 1992.47.1a&b with segmented bones shown inside the semi-transparent blocks, C, segmented bones in preserved position shown enlarged. Scale bar = 10mm.

165x196mm (300 x 300 DPI)

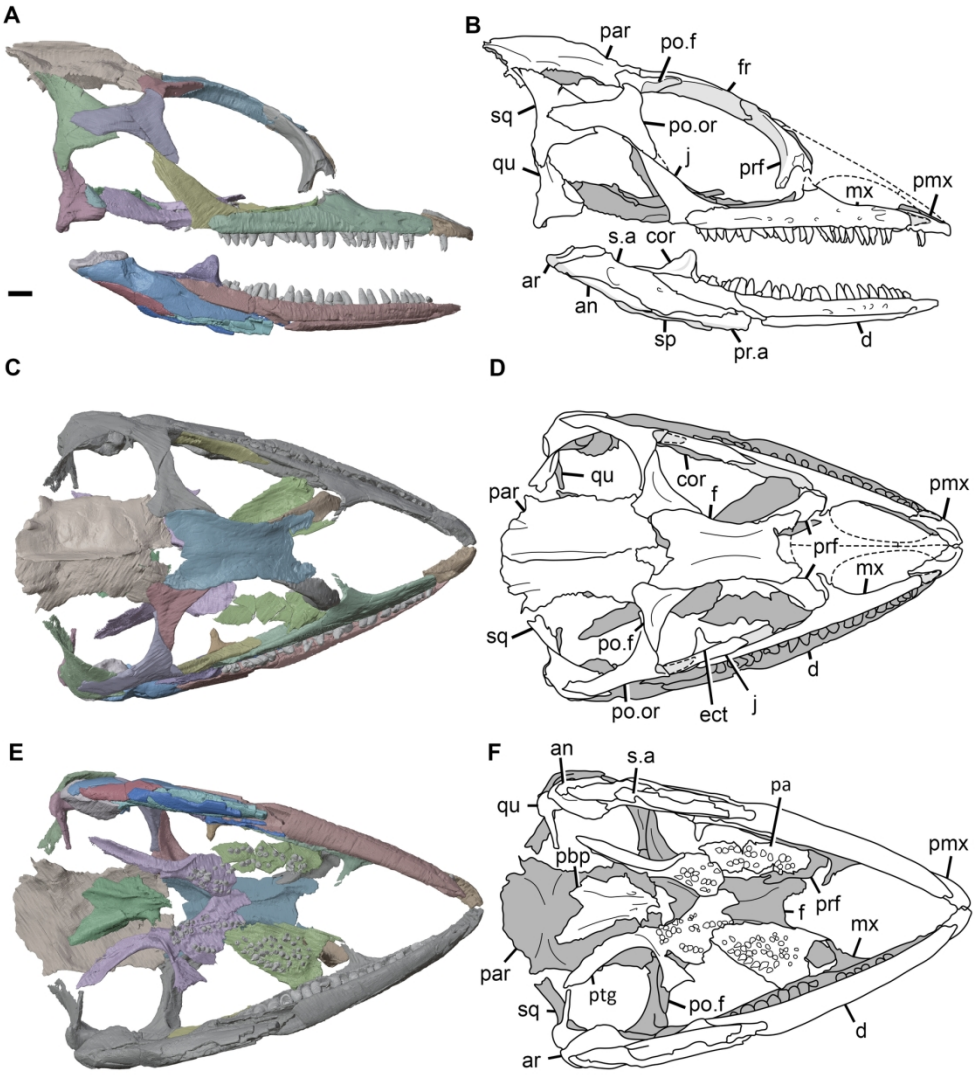

FIG. 2. Digital skull reconstruction of Marmoretta oxoniensis, using information from NMS G 1992.47.1a and CAMSM X9991, in A–B, lateral, C–D, dorsal and E–F ventral views. Grey shading is used in line drawings (B,D,F) to provide information on depth. Abbreviations: an = angular; ar = articular; cor = coronoid; d = dentary; ect = ectopterygoid; fr = frontal; j = jugal; mx = maxilla; pa = palatine; par = parietal; pbp = parabasisphenoid; pmx = premaxilla; po.f = postfrontal; po.or = postorbital; pr.a = prearticular; prf = prefrontal; ptg = pterygoid; qu = quadrate; s.a = surangular; sq = squamosal. Dashed lines indicate broken/restored regions of the cranium. Scale bar = 1mm.

165x190mm (300 x 300 DPI)

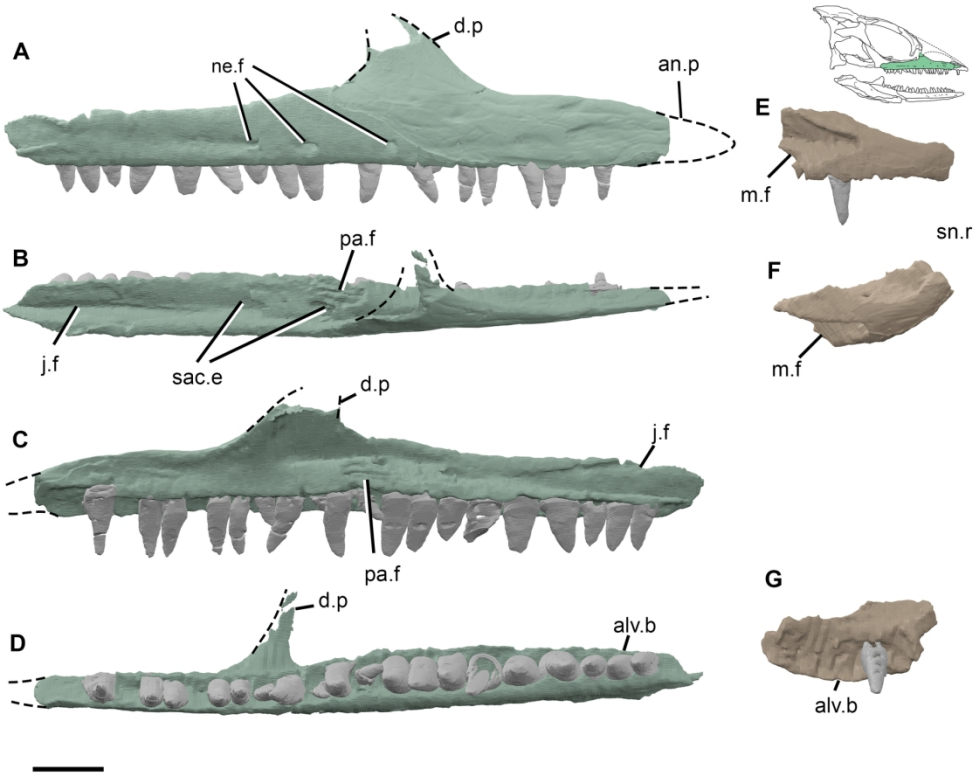

FIG. 3. Marmoretta, Skye, specimen NMS G 1992.47.1a. Right maxilla in A, lateral, B, dorsal, C, medial, and D, ventral views. Right premaxilla in E, lateral, F, dorsal, and G, ventral views. Abbreviations: alv.b = alveolar border; d.p = dorsal process; j.f = jugal facet; m.f = maxilla facet; ne.f = neurovascular foramina pa.f = palatine facet; sac.e = superior alveolar canal entrance; sn.r = subnarial ramus. Dashed lines indicate broken/restored regions of the bone. Scale bar =1mm.

165x136mm (300 x 300 DPI)

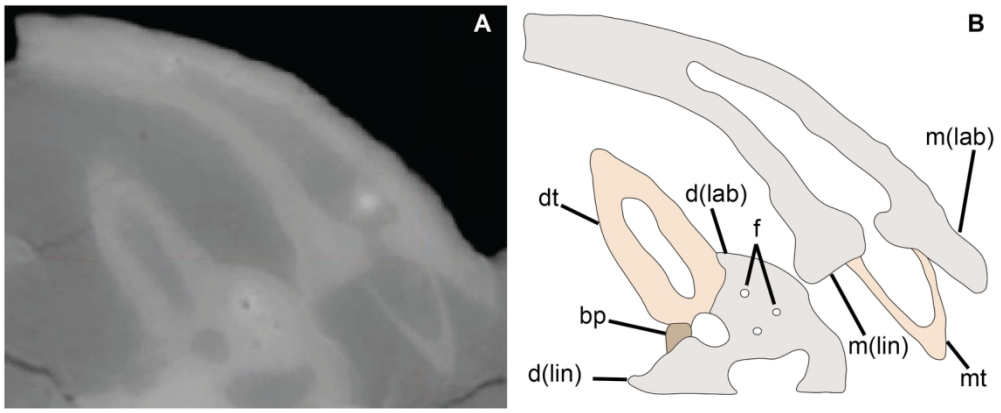

Fig. 4. Marmoretta, Skye, specimen NMS G 1992.47.1a. Cross section (A) and interpretive drawing (B) of tooth implantation in the maxilla and dentary. Abbreviations: bp = basal plate; d(lab) = dentary labial wall; d(lin) = dentary lingual wall; dt = mature dentary tooth; f = nutrient foramina; m(lab) = maxilla labial wall; m(lin) = maxilla lingual wall; mt = emerging maxillary tooth.

144x58mm (300 x 300 DPI)

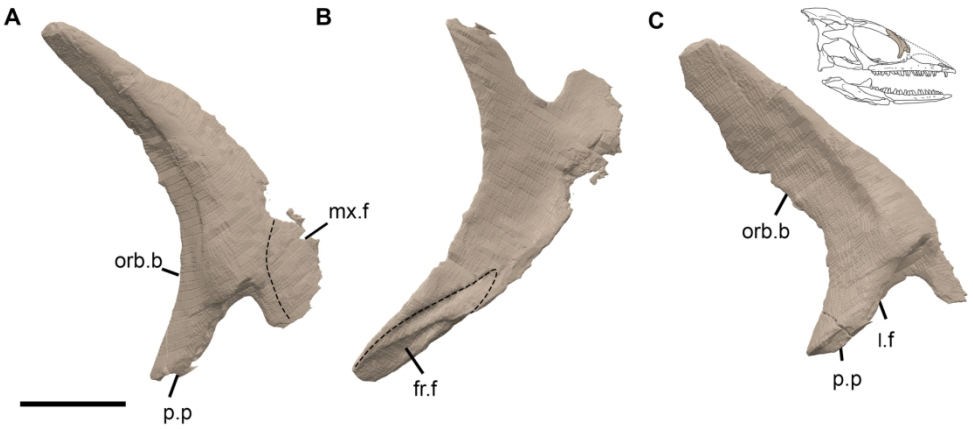

FIG. 5. Marmoretta, Skye, specimen NMS G 1992.47.1a. Right prefrontal in A, dorsal, B, ventral, and C, lateral views. Abbreviations: fr.f = frontal facet; l.f = lacrimal facet; mx.f = maxillary facet; orb.b = orbital border; p.p = palatine process. Scale bar = 1mm.

165x81mm (300 x 300 DPI)

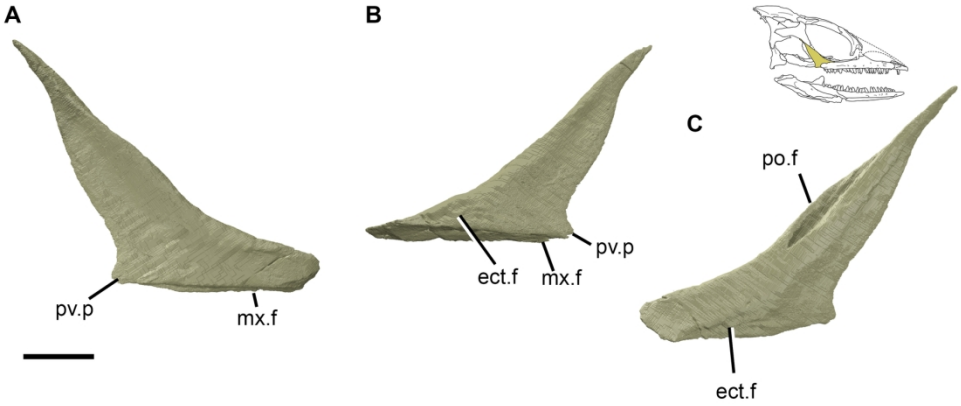

FIG. 6. Marmoretta, Skye, specimen NMS G 1992.47.1a. Right jugal in A, lateral, B, dorsomedial oblique and C, medial views. Abbreviations: ect.f = ectopterygoid facet; mx.f = maxillary facet; po.f = postorbital facet; pv.p = posteroventral process. Scale bar = 1mm.

165x70mm (300 x 300 DPI)

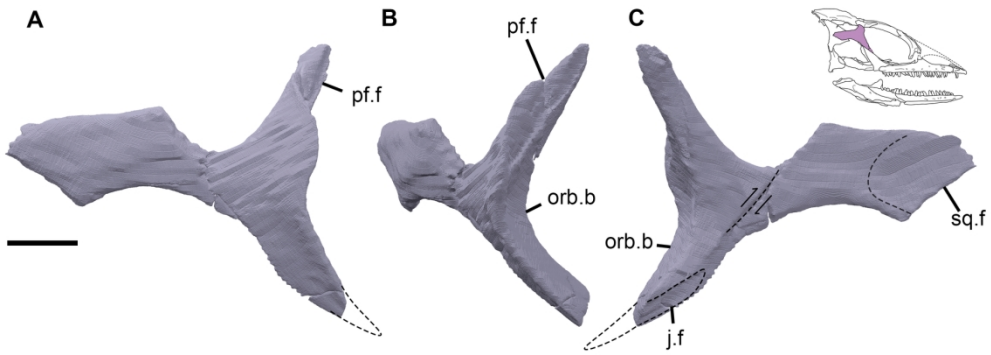

FIG. 7. Marmoretta, Skye, specimen NMS G 1992.47.1a. Right postorbital in A, lateral, B, anterolateral oblique and C, medial views. Abbreviations: j.f = jugal facet; orb.b = orbital border; pf.f = postfrontal facet; sq.f = squamosal facet. Dashed lines indicate broken/restored regions of the bone. Scale bar = 1mm.

165x63mm (300 x 300 DPI)

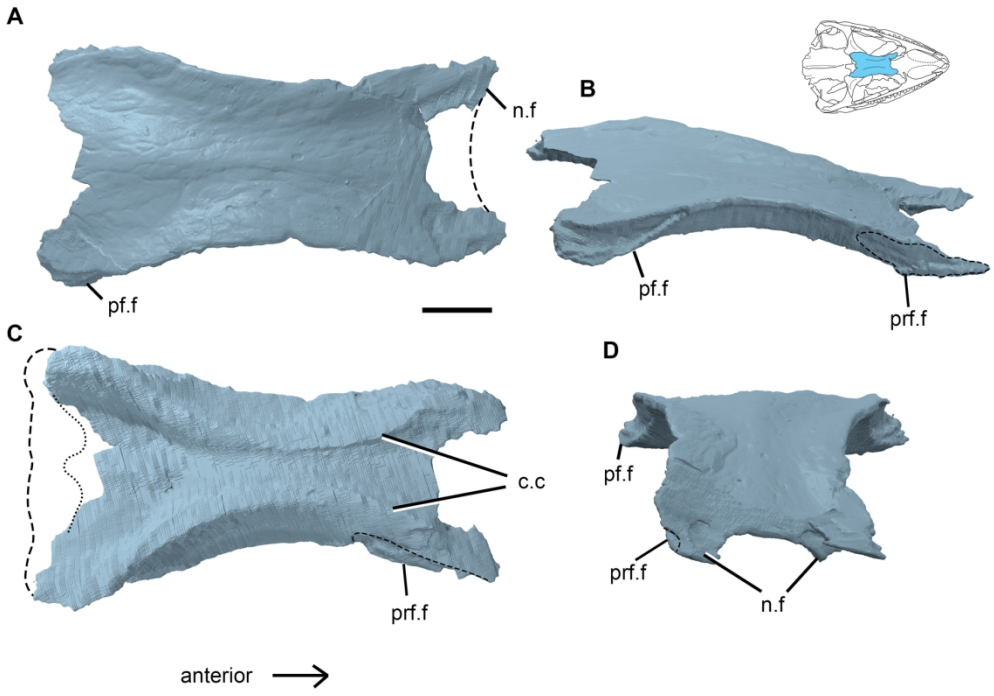

FIG. 8. Marmoretta, Skye, specimen NMS G 1992.47.1a. Frontal in A, dorsal, B, oblique right posterolateral, C, ventral and D, anterodorsal views. Dashed lines show estimated outlines of original bone before breakage, and are used to indicate broken regions. Dotted line in C estimates the ventral portion of the bone. Abbreviations: c.c = cristae cranii; n.f = nasal facet; pf.f = postfrontal facet; prf.f = prefrontal facet. Scale bar = 1mm.

165x125mm (300 x 300 DPI)

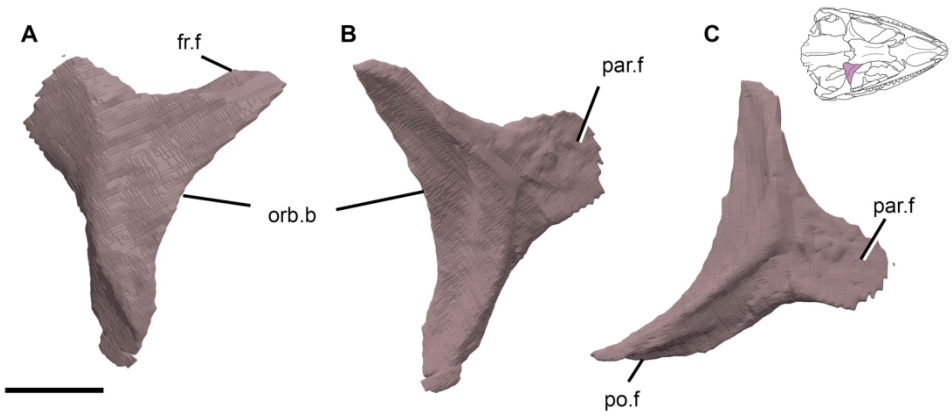

FIG. 9. Marmoretta, Skye, specimen NMS G 1992.47.1a. Right postfrontal in A, lateral, B, medial and C, ventromedial views. Abbreviations: fr.f = frontal facet; orb.b = orbital border; par.f = parietal facet; po.f = postorbital facet. Scale bar = 1mm.

165x76mm (300 x 300 DPI)

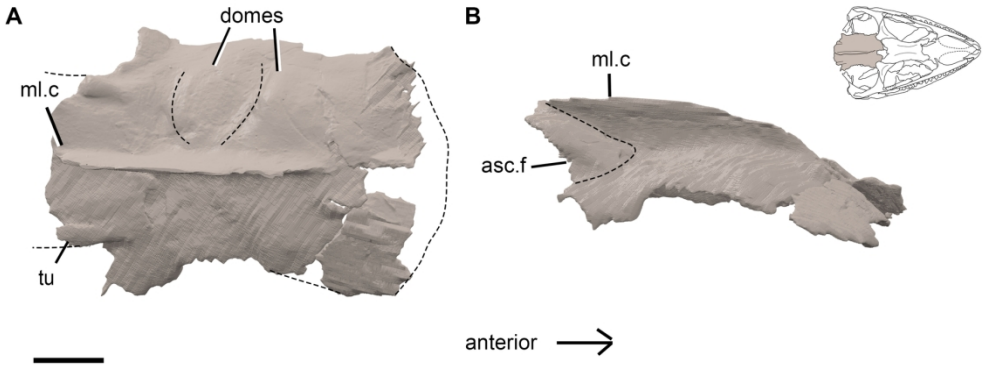

FIG. 10. Marmoretta, Skye, specimen NMS G 1992.47.1a. Parietal in A, dorsal, and B, right lateral views. Abbreviations: acs.f = ascending flange ; ml.c = midline crest; tu = tubercle. Dashed lines are to highlight the depressions between the domes as well as broken/estimated bone outlines. Scale bar = 1mm.

165x71mm (300 x 300 DPI)

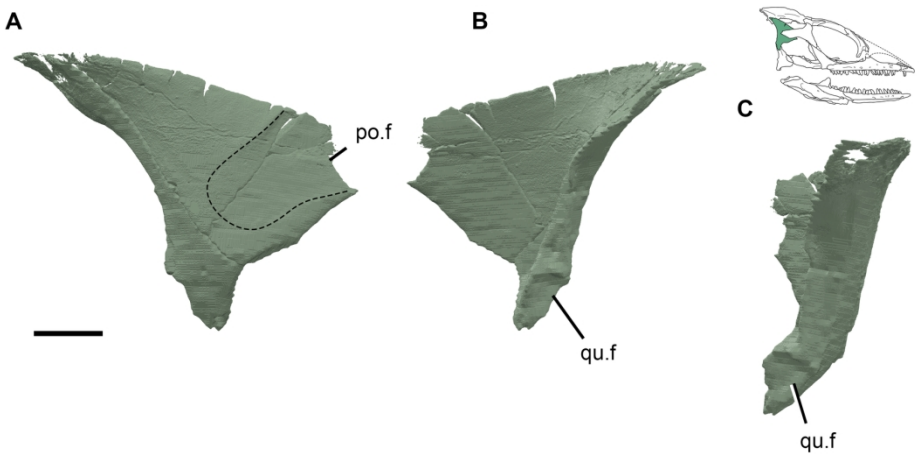

FIG. 11. Marmoretta, Skye, specimen NMS G 1992.47.1a. Right squamosal in A, lateral, B, medial and C, posterior views. Abbreviations: po.f = postorbital facet; qu.f = quadrate facet. Scale bar = 1mm.

165x82mm (300 x 300 DPI)

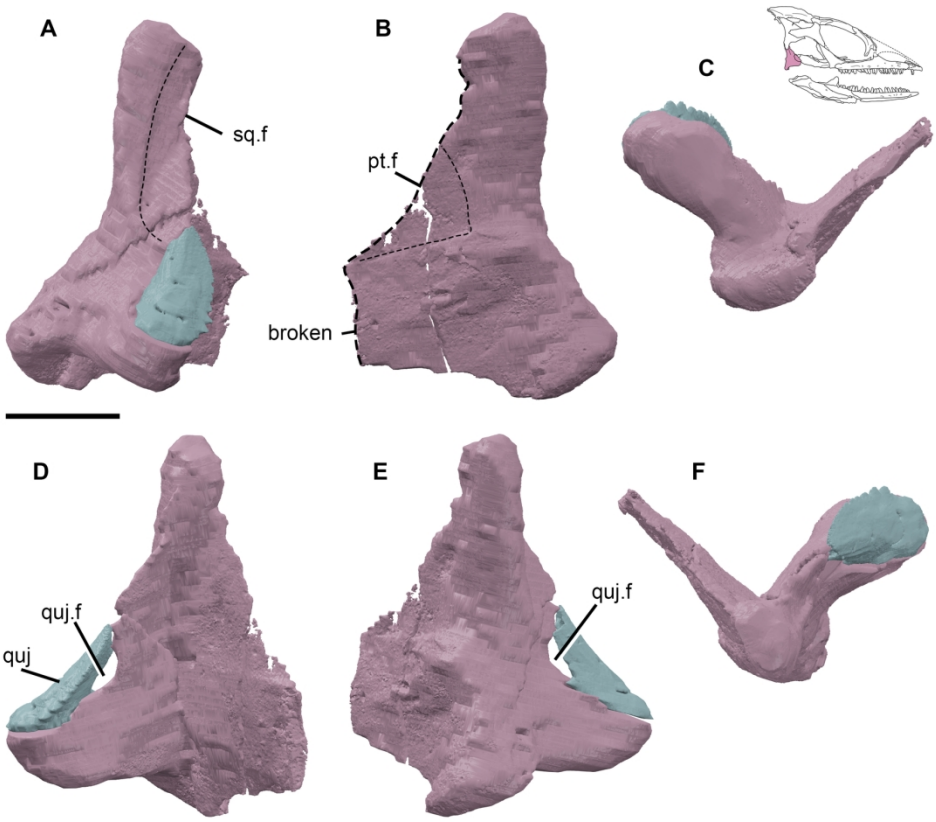

FIG. 12. Marmoretta, Skye, specimen NMS G 1992.47.1a. Right quadrate and quadratojugal in A, lateral, B, medial, C, ventral, D, anterior, E, posterior and F, dorsal views. Abbreviations: pt.f = pterygoid facet; quj = quadratojugal; quj.f = quadratojugal foramen; sq.f = squamosal facet. Dashed lines indicate broken/restored regions of the bone. Scale bar = 1mm.

165x148mm (300 x 300 DPI)

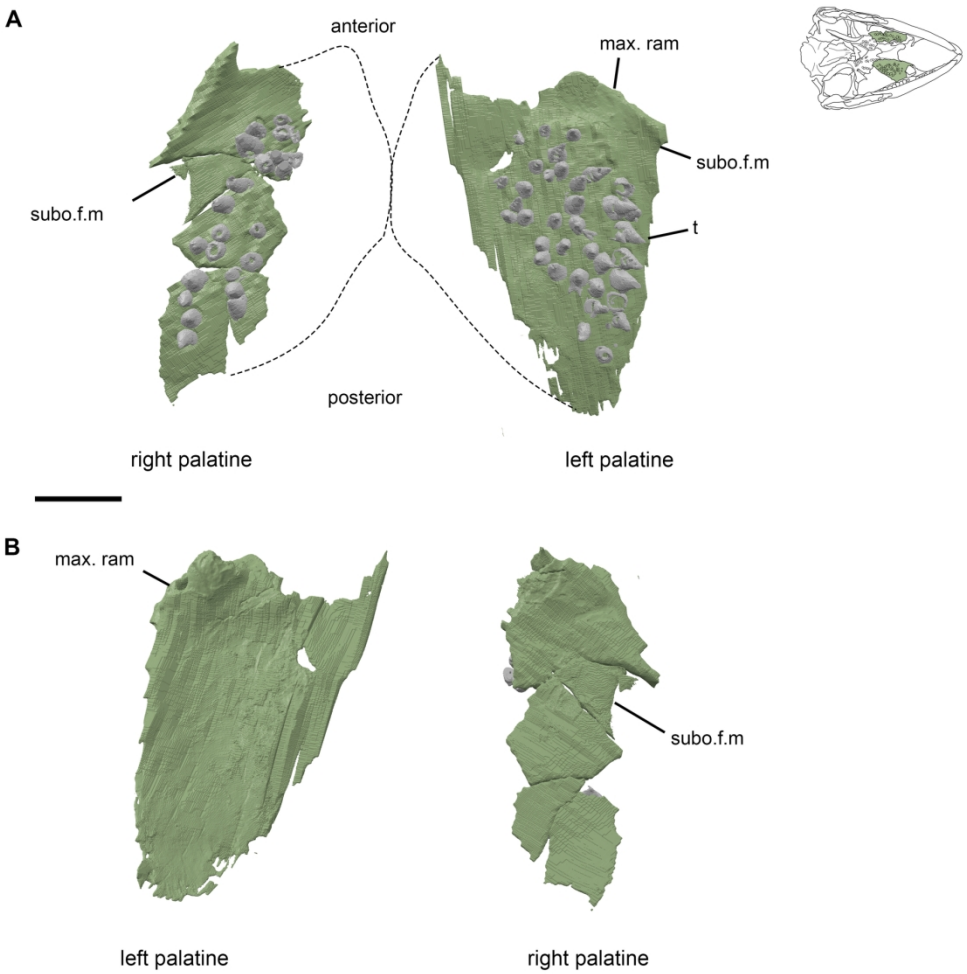

FIG. 13. Marmoretta, Skye, specimen NMS G 1992.47.1a. Left and right palatine in A, ventral view and B, dorsal view. Abbreviations: max. ram = maxillary ramus; subo.f.m = suborbital fenestra margin; t = teeth. Scale bar = 1mm.

165x169mm (300 x 300 DPI)

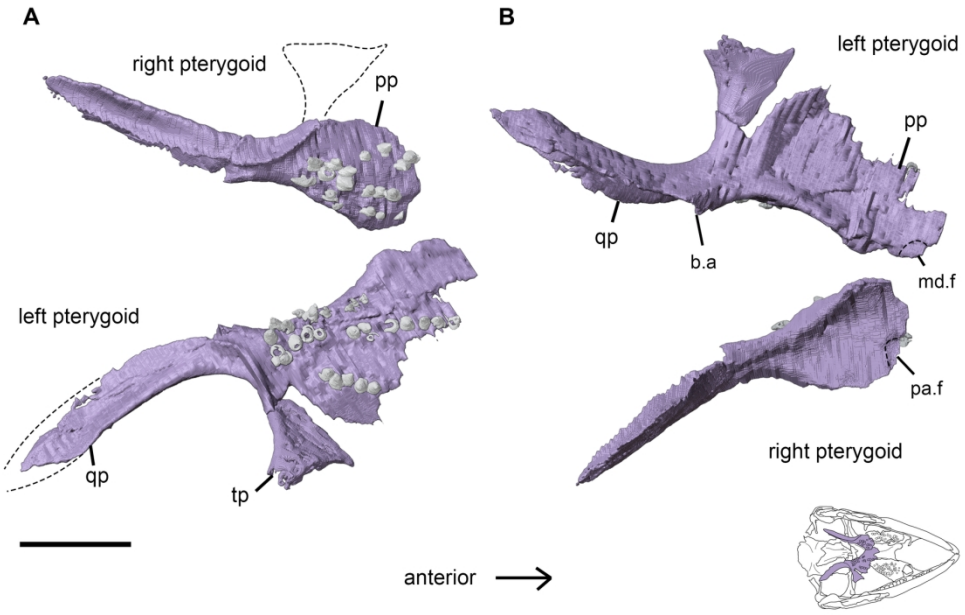

FIG. 14. Marmoretta, Skye, specimen NMS G 1992.47.1a. Left and right pterygoids in A, ventral and B, dorsal views. Abbreviations: b.a = basal articulation; md.f = midline facet; pa.f = palatine facet; pp = palatal plate ; qp = quadrate process; tp = transverse process. Dashed lines indicate broken/restored regions of the bone. Scale bar = 1mm.

165x106mm (300 x 300 DPI)

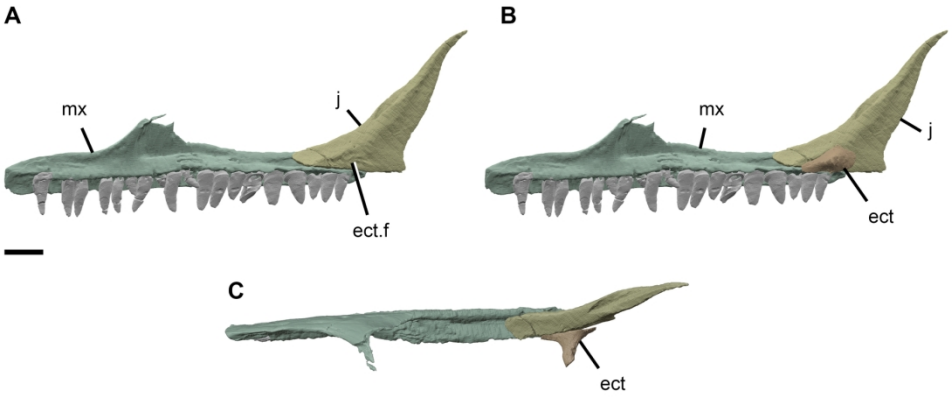

FIG. 15. Marmoretta, Skye, specimen NMS G 1992.47.1a Right maxilla, jugal and ectopterygoid in medial view A without ectopterygoid showing facet on jugal, B with ectopterygoid and C dorsal view. Abbreviations: ect.f = ectopterygoid facet; ect = ectopterygoid; j = jugal; mx = maxilla. Scale bar = 1mm.

165x73mm (300 x 300 DPI)

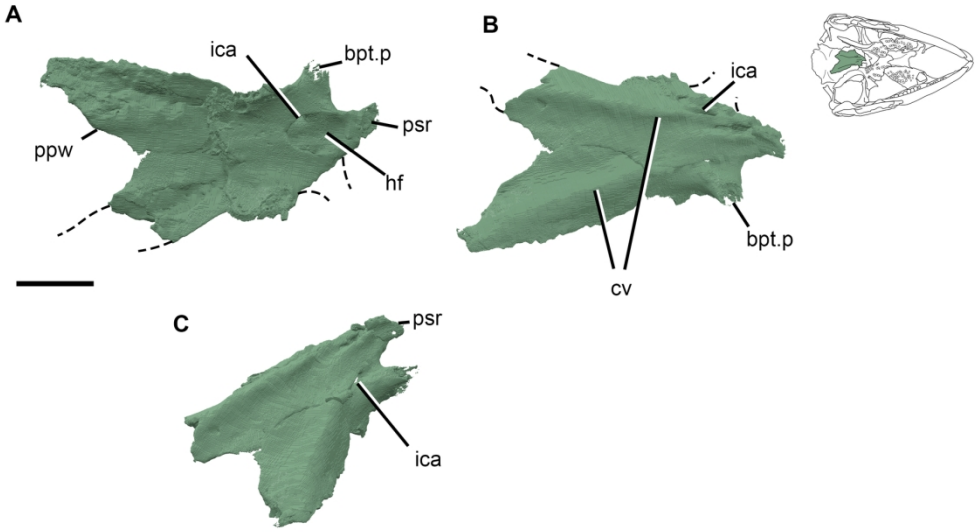

FIG. 16. Marmoretta, Skye, specimen NMS G 1992.47.1a. Parabasisphenoid in A, dorsal, B, ventral and C, posteroventral views. Abbreviations: bpt.p = basipterygoid processes; cv = cristae ventrolaterales; hf = hypophysial fossa; ica = internal carotid foramen; ppw = posterior parasphenoid wing; psr = parasphenoid rostrum. Dashed lines indicate broken/restored regions of the bone. Scale bar = 1mm.

165x93mm (300 x 300 DPI)

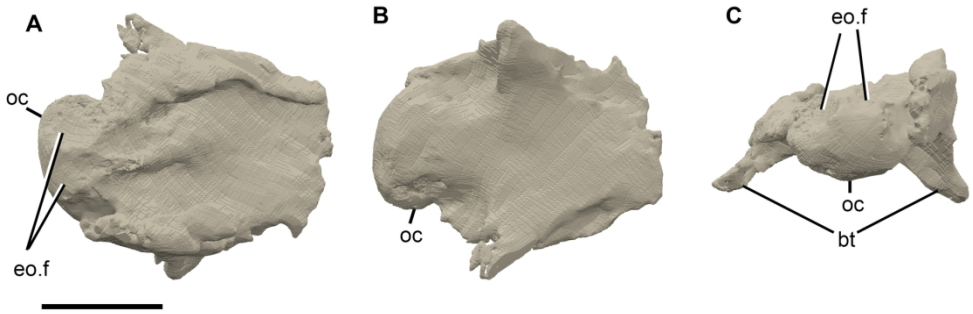

FIG. 17. Marmoretta, Skye, specimen NMS G 1992.47.1a. Basioccipital in A, dorsal, B, ventral and C, posterior views. Abbreviations: bt = basal tubera; eo.f = exoccipital facet; oc = occipital condyle. Scale bar = 1mm.

165x61mm (300 x 300 DPI)

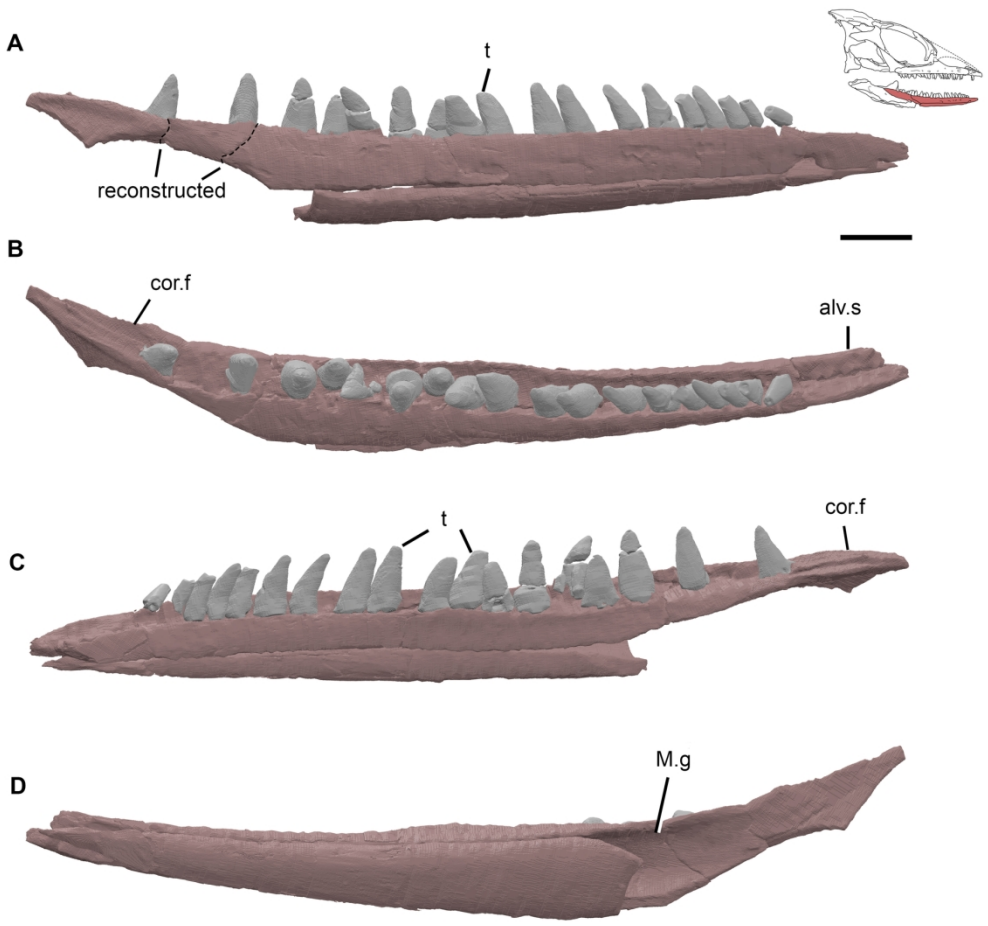

FIG. 18. Marmoretta, Skye, specimen NMS G 1992.47.1a. Right dentary in A, lateral, B, dorsal, C, medial, and D, ventral views. Abbreviations: alv.s = alveolar shelf; cor.f = coronoid facet ; M.f = Meckelian fossa; t = teeth. Scale bar = 1mm.

165x156mm (300 x 300 DPI)

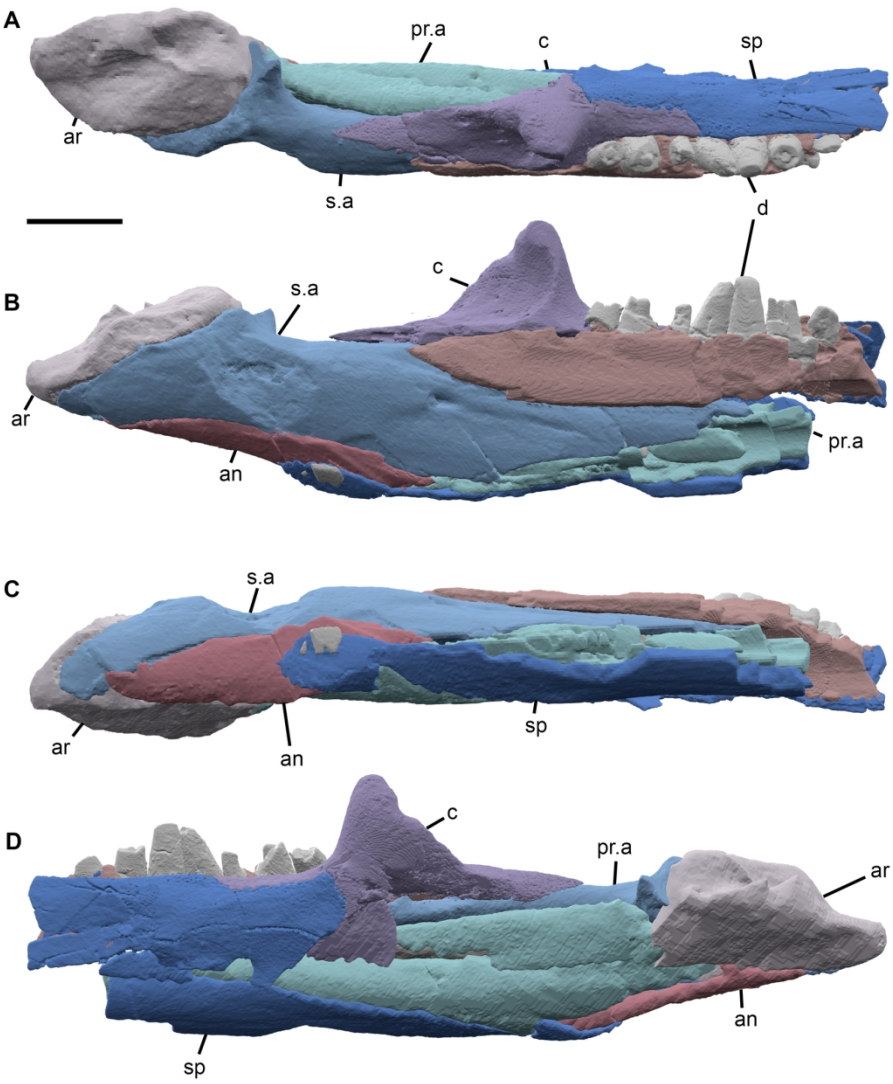

FIG. 19. Marmoretta oxoniensis, referred specimen CAMSM X9991. Right lower jaw approximately as preserved, with slight reconstruction to move the prearticular, splenial and angular into place. A dorsal, B, lateral, C, ventral and D, medial views. Abbreviations: an = angular; ar = articular; c = coronoid; d = dentary; pr.a = prearticular; s.a = surangular; sp = splenial. Scale bar = 1mm.

165x192mm (300 x 300 DPI)

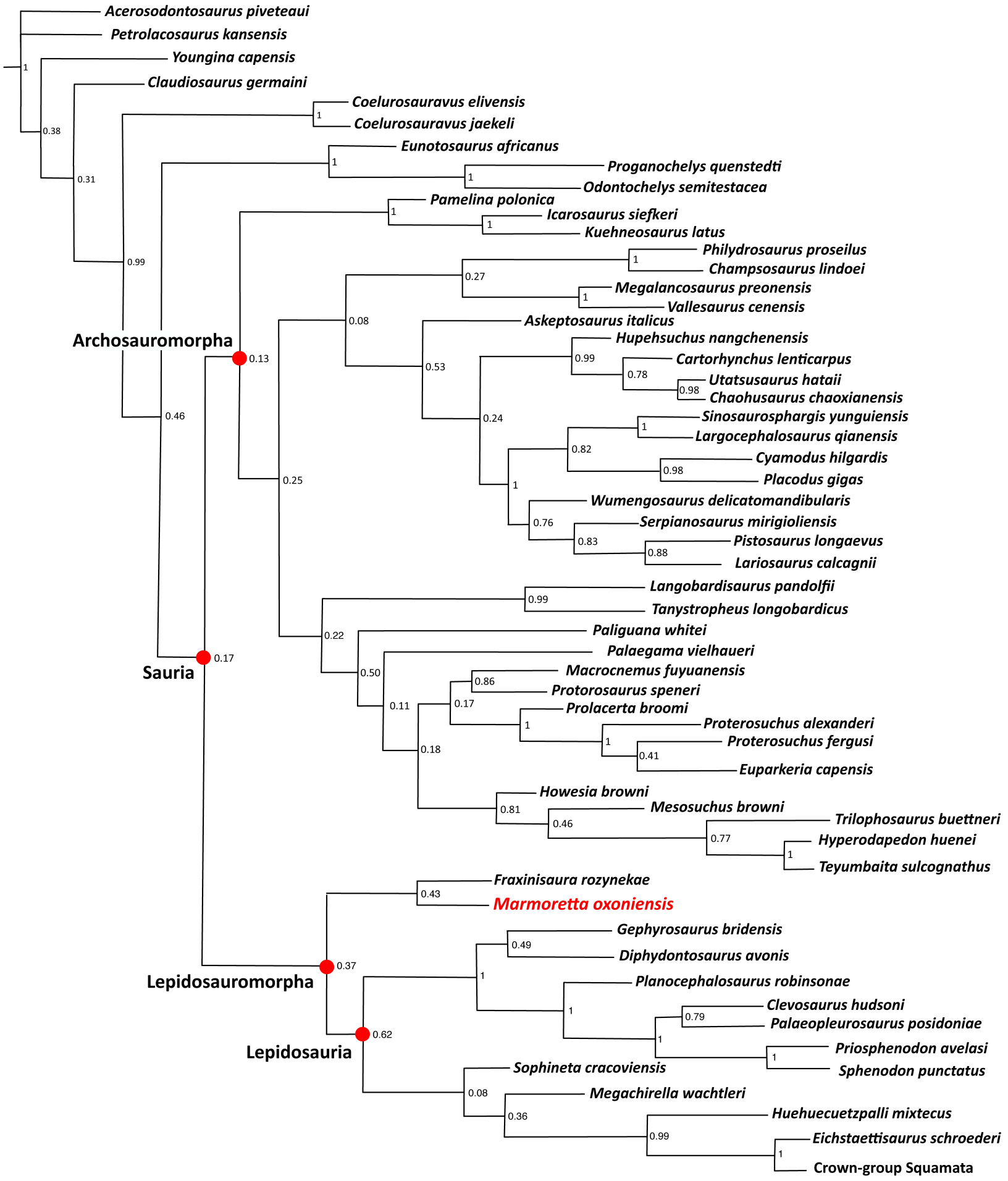
Acerosodontosaurus piveteaui
Petrolacosaurus kansensis
Youngina capensis
Claudiosaurus germaini
Coelurosauravus elivensis
Coelurosauravus jaekeli
Eunotosaurus africanus
Proganochelys quenstedti
Odontochelys semitestacea
Pamelina polonica
Icarosaurus siefkeri
Kuehneosaurus latus
Philydrosaurus proseilus
Champsosaurus lindoei
Megalancosaurus preonensis
Vallesaurus cenensis
Askeptosaurus italicus
Hupehsuchus nangchenensis
Cartorhynchus lenticarpus
Utatsusaurus hataii
Chaohusaurus chaoxianensis
Sinosaurosphargis yunguiensis
Largocephalosaurus qianensis
Cyamodus hilgardis
Placodus gigas
Wumengosaurus delicatomandibularis
Serpianosaurus mirigioliensis
Pistosaurus longaevus
Lariosaurus calcagnii
Langobardisaurus pandolfii
Tanystropheus longobardicus
Paliguana whitei
Palaegama vielhaueri
Macrocnemus fuyuanensis
Protorosaurus speneri
Prolacerta broomi
Proterosuchus alexanderi
Proterosuchus fergusi
Euparkeria capensis
Howesia browni
Mesosuchus browni
Trilophosaurus buettneri
Hyperodapedon huenei
Teyumbaita sulcognathus
Fraxinisaura rozynekae
Marmoretta oxoniensis
Gephyrosaurus bridensis
Diphydontosaurus avonis
Planocephalosaurus robinsonae
Clevosaurus hudsoni
Palaeopleurosaurus posidoniae
Priosphenodon avelasi
Sphenodon punctatus
Sophineta cracoviensis
Megachirella wachtleri
Huehuecuetzpalli mixtecus
Eichstaettisaurus schroederi
Crown-group Squamata
Archosauromorpha
Sauria
Lepidosauromorpha
Lepidosauria
1
0.38
0.31
0.99
1
1
1
1
1
1
0.27
1
0.08
0.53
0.99
0.78
0.98
0.24
1
0.82
0.98
1
0.76
0.83
0.88
0.99
0.22
0.50
0.86
0.11
0.17
1
1
0.41
0.18
0.81
0.46
0.77
1
0.43
0.49
1
1
0.79
1
1
0.08
0.36
0.99
1
0.46
0.13
0.25
0.17
0.37
0.62

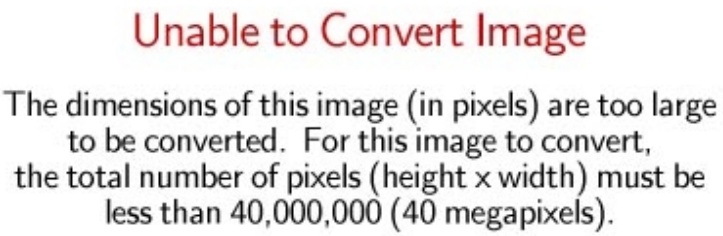

FIG. 20. Maximum clade credibility tree recovered from Bayesian analysis using non-time calibrated Mkv model. Figures adjacent to nodes are the posterior probability value of the node.

PHYLOGENETIC ANALYSIS

We performed a non-time calibrated Bayesian analysis using the Mkv model with the modified and augmented dataset of 377 characters using MrBayes v.3.2.5. The 'standard' datatype was used for morphological data, and the coding was set at 'variable' (that is, only variable characters being sampled) with rates set to a gamma distribution. Gamma distribution modifies the Mkv substitution model to allow variation in the rates of evolution among characters. The Mkv model analysis was performed with two runs of four chains each for 30 million generations, sampling trees every 500th generation with a 25% burn-in. We applied a constraint on the analysis to simulate a molecular backbone for squamates, the details of which are provided in the script for the analysis provided in Supplementary Data. The average effective sample size (ESS) for the two parameters (tree length and shape of gamma distribution) were in excess of 27,000, and the average potential scale reduction factor (PSRF) was 1.000, with both chains demonstrating good convergence (average standard deviation of split frequencies 0.0035). We used a maximum clade credibility tree (Fig. 20) (MCC) to summarize the results of our analysis. The MCC tree is a single tree in the posterior sample with the maximum product of posterior clade probabilities across all the constituent bifurcations (Heled and Bouckarert 2013). We used TreeAnnotator v.1.10.4 (Rambaut and Drummond 2016) to generate the MCC by combining the tree files (.t files) of both runs derived from the MrBayes analysis. The 50% majority-rule tree is also provided in our analysis (halfcompat command in MrBayes) (see Supplementary Data). Optimisation of the state/node distribution of the MCC tree was performed in PAUP v 4.0 for Mackintosh (Swafford 2003) for both delayed transition (deltran) and accelerated transition (acctran).

Compilation of phylogenetic data

A modified and augmented the version of the dataset of 347 morphological characters and 129 taxa complied by Simões *et al.* (2018) was used to determine the phylogenetic position of *Marmoretta*. The modifications and additions made to the dataset are summarised as follows:

Taxon choice

We revised the scores of many taxa and characters, focusing on the basal saurians including *Megachirella, Sophineta, Palaegama, Gephyrosaurus, Diphydontosaurus, Kuehneosaurus* and *Pamelina*. These changes are detailed below, along with some explanatory notes. Our final analysis includes all taxa included in the analysis of Simoes *et al.* (2018) except for several early reptiles that were not relevant to this analysis of the lepidosaur stem, e.g. *Protorothyris*, *Protocaptorhinus*, *Captorhinus*, *Labidosaurus*, *Araeoscelis gracilis*, *Araeoscelis pricei*, *Hovasaurus* and *Saurosternon*. We retained *Petrolacosaurus, Acerosodontosaurus, Youngina* and *Claudiosaurus* to provide outgroup definition. We omitted the marine reptiles *Parvinatator*, *Gulosaurus*, *Mixosaurus*, *Endennasaurus* and *Xinpusaurus,* the stem turtle *Kayentachelys*, the archosauriform *Erythrosuchus* and the tanystropheid *Macrocnemus bessanii* as we did not have detailed observations of these taxa, and their groups are well represented in the remaining taxa. In respect to crown-group lepidosaurs, only *Homeosaurus* and *Kallimodon* were omitted since we were unable to verify the scores based on the available published data, and the specimens were not personally examined. We also added several taxa: the early

lepidosauromorph *Fraxinisaura rozynekae, Chaohusaurus chaoxianensis* and *Cartorhynchus lenticarpus* as representative basal ichthyopterygians, and *Vallesaurus cenensis* as an additional drepanosaur, resulting in a total of 115 operational taxonomic units.

New, modified and deleted characters

We added 32 new characters to the original dataset. Of these, 30 are numbered c.348 to c.377 and are detailed below. Two further new characters replaced the original squamosal characters c.51 (Squamosals, posterior process: absent/present) and c.55 (Squamosal, anterior margin, bifid facet for postorbital: absent/present), and the original c.52 has been renumbered as c.51. Therefore, the two new squamosal characters are detailed below as c.52 and c.55. Otherwise all characters are numbered in accordance with the character list of Simões *et al.* (2018). The wording of eight of the original characters has been modified for clarity or to reflect redundant character states. These characters are also detailed below.

New characters:

52. Squamosal, dorsal process, contact with supratemporal or supratemporal process of parietal: sutured (0) / not sutured, forms a buttress for posterolateral corner of the skull roof (1) – NEW

Notes: the loss of sutural contact between the squamosal and the skull roof is a key modification in the transition to squamate streptostyly (Evans 2008). In many squamates the dorsal process of the squamosal is lost (see c.51), and the squamosal is a narrow and curves posteroventrally ('hockey-stick' shaped, e.g. scincids, lacertids, gymnophthalmids, anguids and varanids – Evans 2008). In some squamates the dorsal process is retained, but this process abuts the parietal or supratemporal rather than making a sutural contact (e.g. in iguanians and some teiids). This character seeks to differentiate between taxa scored for state (1) in c.51 (dorsal process is present), where there is sutural contact of the dorsal process/skull roof (e.g. in non-lepidosaurian lepidosauromorphs and other diapsids) and crown-group squamates where the contact is not sutured allowing cranial kinesis to occur.

55. Squamosal, anterior process, dorsoventral length: narrow, < one-quarter of the dorsoventral length of the postorbital region (0) / deep, > one-third of the dorsoventral length of the postorbital region (1) - – NEW

Notes: Contact between the anterior region of the squamosal and the dorsal process of the jugal occurs in rhynchocephalians and several squamates (see Gauthier et al. 2012 c.154). However, in rhynchocephalians this contact is due to a dorsoventrally deep region of the squamosal, rather than an elongate dorsal process of the jugal. This region, along with the postorbital, forms a thick lower bar of the upper temporal fenestra present in rhynchocephalians. This character seeks to identify this morphology as synapomorphy of rhynchocephalians, which is independently present in several secondarily marine taxa.

348. Skull proportions: preorbital skull length equal to postorbital length (0) / preorbital length exceeds postorbital skull length (1) / postorbital length exceeds preorbital skull length (2) (modified from Gauthier *et al.* 1988 ch.44; Rieppel and de Braga 1997 ch.19, Reisz *et al.* 2010 ch.6, Benson 2012 ch.2, Modesto et al 2015 ch.47, Ford and Benson 2020 ch.1).

Note: In early diapsids, with few exceptions (e.g. rhynchosaurs), the preorbital region of the skull is longer than the postorbital region (state 1). This condition is also found in early lepidosauromorphs (e.g. *Marmoretta, Sophineta* and *Fraxinisaura*) as well as early rhynchocephalians (e.g. *Gephyrosaurus*, *Diphydontosaurus* and *Planocephalosaurus*). However, in derived rhynchocephalians and many squamates the postorbital region is longer than the preorbital (state 2), or both regions are of similar length (state 0).

349. Prefrontal/palatine antorbital contact: absent (0) / narrow forming less than 1/3 the transverse distance between the orbits (1) / contact broad, forming at least 1/2 the distance between the orbits (2) (modified from Laurin and Reisz 1995 ch.6 and 7; Rieppel and deBraga 1997 ch.20, Müller 2004 ch.130, Modesto et al. 2015 ch.12 and 13, Ford and Benson 2020 ch.56 and 57)

Note: In squamates the ventral region of the prefrontal contacts the maxillary process of the palatine, forming either a narrow (state 1) or broad (state 2) medial contact. In early diapsids the contact is either absent (state 0) or, if present, narrow (state 1).

350. Postfrontal contribution to upper temporal fenestra: postfrontal excluded (0) / postfrontal included (1) (from Rieppel and deBraga 1997 ch. 29)

Note: The exclusion of the postfrontal from the upper temporal fenestra in diapsids is considered the plesiomorphic condition. This morphology was present in early diapsids (e.g. *Petrolacosaurus*, *Claudiosaurus* and *Youngina*), in early archosauromorphs (e.g. *Protorosaurus* and *Prolacerta*), in archosauriforms (e.g. *Proterosuchus* and *Euparkeria*) and kuehneosaurs. In *Marmoretta*, *Sophineta* and all lepidosauromorphs where the postfrontal is not fused to the postorbital, the postfrontal participates in the upper temporal opening (state 1).

351. Angular lateral exposure: exposed along 1/3 of the lateral face of the mandible (0) / exposed only as a small sliver along the lateral face (1) (from Rieppel and deBraga 1997 ch.20)

Note: In early diapsids and most archosauriforms the angular has extensive exposure in lateral view (state 0). In *Marmoretta* and many lepidosauromorphs, including all rhynchocephalians, the angular is reduced to a dorsoventrally narrow exposure in the lateral surface of the mandible (state 1). The derived condition was considered a synapomorphy of lepidosauromorphs (Rieppel and deBraga 1997), with convergence in rhynchosaurs (e.g. *Mesosuchus*).

352. Maxilla orbital exposure: absent (0) / present (1) (from Rieppel and deBraga 1997 ch.15)

Note: In many early diapsids, the maxilla is prevented form contributing to the orbital margin (state 0) by contact between the lacrimal and jugal. In kuehneosaurs and non-lepidosaurian lepidosauromorphs, the maxilla contributes to the anteroventral region of the orbit (state 1). The derived state is also present in rhynchocephalians and some squamates, although reversed in some squamate groups (e.g. iguanians and agamids).

353. Maxilla length: extends at least to the posterior orbital margin (0) / does not reach posterior margin of orbit (1) (from Rieppel and deBraga 1997 ch.14, Müller 2004, Ezcurra et al. 2014 c.122, Ford and Benson 2020 ch.41)

Note: An elongate suborbital process of the maxilla is present in basal testudines (e.g. *Eunotosaurus* and *Proganochelys*), some rhynchosaurs and archosauriforms (e.g. *Proterosuchus* and *Euparkeria)*(state 0). In all non-lepidosaur lepidosauromorphs and squamates, with the exception of

snakes and some amphisbaenians, the suborbital process of the maxilla is short and does not extend to the posterior margin of the orbit (state 1).

354. Frontal, morphology: parallelogram shaped (0) / hour-glass shaped (1) (from Rieppel and deBraga 1997 ch.27)

Note: the plesiomorphic state of the paired frontals in amniotes are take the form of a parallelogram when view dorsally (state 0). Mid-length constriction of the frontals resulting in a hourglass shape morphology (state 1) is found in most saurians, with the exception of some rhynchosaurs, snakes and amphisbaenians.

355. Dorsal vertebrae, transverse processes: short no more than the total transverse width of the neural arch (0) / long exceeding the transverse width of the neural arch (1) (modified from Laurin 1991 F.5, Rieppel and deBraga 1997 ch.108, Reisz et al. 2010 ch.75, Benson 2012 ch.158, Ezcurra 2016 ch.358, Ford and Benson 2020 ch.201)

Note: In early diapsids the transverse processes of the dorsal vertebrae are short (state 0) (e.g. *Petrolacosaurus, Youngina, Acerosodontosaurus*). In many archosauromorphs and kuehneosaurs, the transverse processes are elongate (state 1). All lepidosauromorphs possess short transverse processes (state 0).

356. Pterygoid, orientation of transverse flange: directed predominantly laterally or posterolaterally (0) / oriented in an anterolateral direction (1) (modified from Laurin and Reisz 1995 ch.45, Rieppel and deBraga 1997 ch.108, Müller 2004 ch.140, Maddin 2008 ch.37, Benson 2012 ch.118, Pritchard et al. 2015 ch.53, Ford and Benson 2020 ch.137)

Note: All non-lepidosaur lepidosauromorphs and rhynchocephalians share the plesiomorphic condition (state 0), as do most non-lepidosauromorph diapsids, with the exception of *Claudiosaurus*, choristoderans and some marine taxa. Many squamates have an anterolaterally directed transverse flange, including the basal squamates *Huehuecuetzpalli* and *Eichstaettisaurus* (state 1).

357. Humerus, torsion: proximal and distal end are off-set at an angle of at least 45°(0) / off set is reduced to no more than 20° (1) (Rieppel and deBraga 1997 ch.123)

Note: Primitively, the proximal and distal epiphyses of the humerus are offset by at least 45° in relation to each other (state 0). In some taxa the offset may be as much as 90° (e.g. *Youngina* and *Claudiosaurus*). In many squamates, including early members such as *Ardeosaurus, Eichstaettisaurus* and *Huehuecuetzpalli* the humeral torsion is reduced (state 1). The derived condition is also found in testudines and sauropterygians.

358. Mandible, adductor chamber: small, quadrate does not extend well below level of occipital condyle (0) / enlarged adductor chamber, and quadrate extends well below occipital condyle (1) (from Gauthier *et al.* 1988a ch.17)

Note: In many squamates (with the exception of snakes, dibamids and amphisbaenians) and in sphenodontians (e.g. *Priosphenodon* and *Sphenodon*) the adductor chamber is enlarged (state 1). The derived condition is considered a synapomorphy of lepidosauromorphs and kuehneosaurs (Gauthier *et al.* 1988)

359. Metacarpals, length of third and fourth: fourth metacarpal longer than third (0) / third and fourth metacarpals subequal in length (1) / fourth metacarpal shorter than third (2) (from Gauthier *et al.* 1988a ch.105)

Note: In early diapsids, metacarpals I to IV increase in length (state 0), with metacarpal V being shorter than metacarpal I. This condition is also found in *Megachirella* and the early squamate *Eichstaettisaurus*. In other squamates generally, metacarpal IV is reduced, and is either subequal to (state 1) or shorter than (state 2) metacarpal III. Exceptionally in drepanosaurs and some archosauromorphs (e.g. *Tanystropheus* and *Euparkeria*) metacarpal IV is also shorter than metacarpal III (state 2). The derived condition (state 2) is considered a synapomorphy of lepidosaurs (Gauthier et al. 1988).

360. Lacrimal, size: large, with an anterior or posterior (suborbital) process which is longer anteroposteriorly than the dorsoventral length of the lacrimal in lateral view (0): small, dorsoventral length greater than anteroposterior length and confined to the orbital rim (1) (from Gauthier *et al.* 1988a ch.1)

Note: Ancestrally, diapsids possess a large lacrimal that extends along the snout, and in some early diapsids contacts the external naris (e.g. *Petrolacosaurus*). Plesiomorphically, therefore, the anteroposterior length of the lacrimal is greater than the dorsoventral length (state 0). This condition is also present in archosauromorphs and marine taxa. The exception to this, in non-lepidosauromorph diapsids, can be found in drepanosaurs and coelurosauravids. In all lepidosauromorphs, the lacrimal, where present, is greatly reduced anteroposteriorly, and often limited to a small bone confined to the orbit rim (state 1). In many squamates, the lacrimal is absent (a condition addressed in c.27). A reduced lacrimal is considered a synapomorphy of lepidosaurs (Gauthier et al. 1988).

361. Fibula, articulation with femur: fibula/femur articulation end to end (0) / fibula sits in a recess on lateral margin of distal end of femur (1) (modified from Gauthier *et al.* 1988a ch.124)

Note: In most diapsids the proximal epiphysis of the fibula meets the distal epiphysis of the femur in a straight end-to-end contact (state 0). All limbed squamates, with few exceptions (e.g. *Pachyrachis* and *Xenosaurus*), share a derived condition, where the proximal epiphysis of the fibula is flattened and pointed, and fits into a recess on the dorsal surface of the distal epiphysis of the femur (state 1).

362. Palatine, lateral row of enlarged teeth: absent (0) / lateral tooth row present on palatine, converging posteriorly (1) (Evans 1980, Gauthier *et al.* 1988a ch.124)

Note: Rhynchocephalians possess a conspicuously enlarged row of teeth on the dorsolateral surface of the palatine (state 1). Snakes often have a single row of large teeth on the palatine, but this is not homologous with that found in rhynchocephalians.

363. Dentary, posterior extent: extends posteriorly no further than the level of coronoid eminence or slightly beyond (0) / extends posteriorly more than halfway between coronoid eminence and articular condyle (1) (from Gauthier *et al.* 1988a ch.66)

Note: All rhynchocephalians possess a posterior process or the dentary that extends well beyond the coronoid eminence and terminates close to the articular condyle (state 1). This was recovered as a synapomorphy of Rhynchocephalia (Gauthier *et al.* 1988)

364. Ectopterygoid, contact with maxilla: absent (0) / present (1) (Dilkes 1988 ch.40, Müller 2004 ch.94, Ezcurra 2016 ch.206, Ford and Benson 2020 ch.146)

Note: In many early diapsids (e.g. *Petrolacosaurus, Claudiosaurus, Eunotosaurus* and *Prolacerta*), the ectopterygoid is restricted to contact with the jugal laterally (state 0). This is also the case in non-lepidosaur lepidosauromorphs (e.g. *Marmoretta* and *Sophineta*). Contact between the ectopterygoid and maxilla (state 1) is found in lepidosaurs, with few exceptions (e.g. *Planocephalosaurus, Elgaria* and *Heloderma*). It is also present convergently in choristoderans, rhynchosaurs, saurosphargids, placodonts and some archosauriforms (e.g. *Trilophosaurus*).

365. Vertebrae, cervical and/or dorsal, anterior centrodiapophyseal or paradiapophyseal lamina: absent (0) / present (1) (from Brinkman and Eberth 1983 ch.17, Ezcurra 2016 ch.315, Ford and Benson 2020 ch.215)

Note: The dorsal vertebrae in many archosauromorphs, apart from rhynchosaurs, display a conspicuous lamina that extends anteroventrally from the base of the transverse process to the anterodorsal corner of the centrum or the anteroventral base of the neural arch (state 1). This is absent (state 0) in non-saurian diapsids and lepidosauromorph.

366. Vertebrae, posterior cervical and/or dorsal, prezygodiapophyseal lamina: absent (0) / present (1) (from Ezcurra 2016 ch.317)

Note: The prezygodiapophyseal lamina connects the base of the transverse process to the lateral margin of the prezygopophysis, and is present (state 1) in many archosauromorphs, although absent in rhynchosaurs. It is also absent (state 0) in non-saurian diapsids and lepidosauromorphs.

367. Jugal, anterior suborbital extension: broadly separated from prefrontal or posterior to the midpoint of the orbit (0) / reaches level of prefrontal or anterior margin of orbit (1) (modified from deBraga and Rieppel 1997 ch.33, Ezcurra 2016 ch.95, Gauthier *et al.* 2012 ch.144)

Note: The suborbital process of the jugal is does not approach the anterior margin of the orbit and is broadly separated from the ventral process of the prefrontal (state 0) in several early diapsids (e.g. *Petrolacosaurus, Claudiosaurus* and *Coelurosauravus*), kuehneosaurs, rhynchocephalians and non-lepidosaur lepidosauromorphs (e.g. *Megachirella, Marmoretta* and *Sophineta).* In many squamates, including early members (e.g. *Ardeosaurus, Eichstaettisaurus* and *Huehuecuetzpalli*) the anterior process is elongate and contacts the prefrontal (state 1). The derived state was recovered as an unambiguous synapomorphy of the clade *Huehuecuetzpalli* + Squamata (Gauthier *et al.* 2012).

368. Basioccipital, articular surface of the occipital condyle: concave (0) / hemispherical (1) (Ezcurra 2016 ch.229)

Note: In early diapsids (e.g. *Petrolacosaurus, Youngina, Coelurosauravus* and *Hovasaurus*) and convergently in rhynchocephalians, the articular surface if the occipital condyle bears a distinct concavity (state 0). The occipital condyle of archosauromorphs bears a convex surface (state 1).

369. Jugal, lateral exposure below orbit: absent (0) / partly exposed above orbital margin of maxilla (1) /entirely exposed above orbital margin of maxilla (2) (Gauthier *et al.* 2012 ch.149)

Note: In many early diapsids, including non-lepidosaur lepidosauromorphs (e.g. *Marmoretta*), the suborbital process of the jugal is partially obscured in lateral view by the overlying posterior process of the maxilla (state 1). In a few cases, such as *Sphenodon* and *Cordylus*, the suborbital process is entirely obscured (state 0). In many squamates (e.g. basal squamates *Ardeosaurus, Eichstaettisaurus* and *Huehuecuetzpalli* and extant agamids, iguanians and monitors) the anterior process of the jugal is fully

exposed in lateral view (state 2). State 2 is also present independently in early ichthyosauriforms, thalattosaurs and choristoderans and some rhynchosaurs. This condition (state 2) was recovered as an unambiguous synapomorphy of the clade *Huehuecuetzpalli* + Squamata (Gauthier *et al.* 2012).

370. Manus, penultimate phalanges: shorter than or equal to antepenultimate (0) / longer than antepenultimate (1) (Gauthier *et al.* 2012 ch.546)

Note: State (0) is present in early diapsids (e.g. *Petrolacosaurus* and *Youngina*) and archosauromorphs. In many lepidosauromorphs, including *Marmoretta, Palaeopleurosaurus*, geckotids and scincomorphs, the penultimate phalange of the manus is longer than the antepenultimate (state 1). This condition is also present independently in drepanosaurs. The derived condition was recovered as an unambiguous synapomorphy of Squamata (Gauthier *et al.* 2012).

371. Jugal, posteroventral process: short or spur-like, anteroventrally less than 20% of the total ventral length (0) / long, greater than 25% of the total ventral length (1) (modified from Gauthier *et al.*1988b ch.34, deBraga and Rieppel 1997 ch.33, Müller 2004 c.16, Reisz *et al.* 2009 c.49, Benson 2012 ch.75, Ford and Benson 2020 ch.78)

Notes: In early archosauromorphs (e.g. *Protorosaurus* and tanystropheids) and non-saurian diapsids (e.g. *Petrolacosaurus* and *Acerosodontosaurus*) the posteroventral process of the jugal is short relative to the length of the ventral surface of the jugal (state 0). In choristoderans, coelurosauravids, rhynchosaurs and archosauriforms (e.g. *Proterosuchus* and *Euparkeria*) the posteroventral process is relatively long, extending posteriorly into the temporal region. This character is inapplicable to taxa where the posteroventral process is scored as absent (c.36).

372. Jugal, contact with quadratojugal: absent (0) / present (1) (from Nesbitt 2011 ch.70)

Notes: Contact between the jugal and quadratojugal (where present) is almost completely absent (state 0) in lepidosauromorphs (with the exception of some rhynchocephalians and some polyglyphanodont squamates). In choristoderans, rhynchosaurs and archosauriforms the jugal and quadratojugal meet (state 1) to provide a ventral bar to the lower temporal fenestra.

373. Vomers, contact with anterior region of maxilla: absent (0) / present (1) (Dilkes 1998 ch.38)

Notes: In choristoderans and rhynchosaurs the vomer contacts the anteromedial surface of the maxilla (state 1). This contact is absent in most other taxa considered herein. In neochoanate squamates (e.g. *Mabuya, Petracola* and *Dibamus*) there is also contact between the vomer and maxilla. However, this character is not devised to describe the complexities of the neochoanate condition in squamates, and these taxa are scored as (0).

374. Prefrontal, contact with counterpart at midline: absent (0) / present (1) (Dilkes 1998 ch.125)

Notes: Midline contact of the prefrontals (state 1) is a synapomorphy of the choristoderans.

375. Interclavicle, notch on anterior margin: absent (0) / present (1) (Dilkes 1998 ch.97)

Notes: A distinctive notch or concavity on the midline of the anterior surface of the interclavicle (state 1) is present in several archosauromorphs (e.g. *Tanystropheus, Prolacerta, Mesosuchus* and *Proterosuchus*). It is absent in all other taxa where the interclavicle is preserved.

376. Tibia, contact with centrale: absent (0) / present (1) (Dilkes 1998 ch.117)

Notes: The distal epiphysis of the tibia contacts the centrale of the pes (state 1) in some archosauromorphs (e.g. *Langobardisaurus, Macrocnemus* and *Prolacerta*), drepanosaurs, rhynchosaurs (e.g. *Mesosuchus*) and archosauriforms (e.g. *Proterosuchus*). It is absent in lepidosauromorphs (state 0).

377. Premaxilla, contact with prefrontal: absent (0) / present (1) (Dilkes 1998 ch.7)

Notes: Contact between the premaxilla and prefrontal (state 1) is a synapomorphy of rhynchosaurs.

Modified characters (changes underlined):

23. Nasals, anterolateral process: absent (0) / present (1)

41. Quadratojugal, ornamentation, on external surface: absent (0) / present (1).
Note: in the revised matrix only two states of the original four were scored. Therefore this character has been changed to binary.

61. Postfrontals, concavity between the frontal and parietal processes (dorsomedial margin of postfrontal): absent (0) / present (1)

108. Pterygoids, transverse process: posteroventrally orientated (0) / flat, on same plane as the posterior region of the palatal ramus of the pterygoid (1)

116. Epipterygoid, base shape: base flared out (0) / base columnar, inserting into a pit on the surface of the pterygoid (1)

119. Quadrates, pterygoid process: present as broad, overlapping quadrate/pterygoid suture (0) / absent or reduced to a small lappet on the ventromedial surface of the quadrate (1)

122. Quadrates, posterodorsal suprastapedial recess with ventrally directed 'hook-like' process: absent (0) / present (1)

309. Humeri, entepicondyle foramen: absent (0) / present (1). Note: This character has been simplified from four to two states.

Changes to the coding of character states

The changes made to the coding of the character states for each taxon, where applicable, are as follows:

Petrolacosaurus
Data sources – Literature: Reisz 1981. Specimens examined: KUVP 1424, 8351, 9951, 9952, 9957, 9958, 33603

10: ? → 0
11: ? → 1
16: ? → 1
23: - → 0
30: ? → 1

33: 0 → 1 (Simoes et al. 2018 score a crest or thickening of the prefrontal on the anterodorsal margin of the orbit as absent (0). However, The prefrontal is heavily thickened at the anterodorsal angle of orbit (see Reisz 1981 p.15))
39: ? → 0
70: 0 → - (since the subolfactory processes are scored as absent (Simoes *et al.* 2018 c.69), the absence or presence of fusion between them should therefore be scored as inapplicable)
111: 1 → 0 (Simoes et al. 2018 score the arcuate flange of the quadrate ramus of the pterygoid as present (1). However, the ventral margin of the quadrate ramus, although thickened, does not form an arcuate flange (see Reisz 1981 p.23)
115: ? → 0
116: ? → 0
155: 1 → ? (Simoes at al. 2018 score the dorsal process of the stapes as present (1). However, the proximal region of the stapes is poorly preserved and the dorsal process cannot be unequivocally defined as present (see Reisz 1981 p.26))
156: ? → 0

Eunotosaurus:
70: 0 → - (since the subolfactory processes are scored as absent (Simoes et al. 2018 c.69), the absence or presence of fusion between them should therefore be scored as inapplicable)

Proganochelys:
Data sources – Literature: Gaffney and Meeker 1983, Gaffney 1990, Bever et al. 2015.

23: 1 → 0 (This character is based on the 'supranarial' process of Gauthier *et al.* 2012 (c.22) where a anterolateral process of the nasal bone extends to contact the lateral margin of the eternal naris. This morphology is not homologous with *Proganochelys* (see Gaffney 1990))
26: 1 → 0 (Gaffney (1990 p.31) notes that the ventral surface of the nasal in *Proganochelys* has a low parasagittal ridge defining the lateral limits of the sulcus olfactorius, rather than the ventromedial crest present in some squamates as inferred by the scoring of this character in Simoes *et al.* 2018)
41: 2 → 1 (This character has been modified to binary states – see note on c.41 above)
70: 0 → - (since the subolfactory processes are scored as absent (Simoes et al. 2018 c.69), the absence or presence of fusion between them should therefore be scored as inapplicable)
113: 1 → 0 (Simoes et al. 2018 score the ectopterygoid as present (1). Gaffney and Meeker (1983) note the ectopterygoid is absent in *Proganochelys*. Gaffney (1990) does not mention or illustrate the ectopterygoid. Bever et al. (2015) score as the ectopterygoid as absent (state 1) in their matrix.)
169: 0 → ? (Simoes et al. 2018 suggest in this character and in characters 202-218 (see below) that *Proganochelys* possesses marginal dentition. However, as Gaffney (1990) notes, *Proganochelys* does not possess marginal dentition (see pp.59,61,67,90 and pers.comm. S. Evers 2020). Consequently, all scores pertaining to marginal dentition have been rescored as inapplicable)
202: ? → -
203: ? → -
204: ? → -
205: ? → -
206: ? → -
207: ? → -
208: ? → -
209: ? → -
210: 0 → -
211: 0 → -
212: 2 → -
213: 2 → -

214: ? → -
215: 0 → -
216: 0 → -
217: ? → -
218: ? → -

Claudiosaurus:
Data Source – Literature: Carroll 1981. Specimens examined: MNHN 1978-6-1/2

39: ? → 0
42: ? → 0
108: 0 → 1(This character has been revised (see above) - Carroll (1981) notes *Claudiosaurus* lacks a ventrally directed transverse flange, but that the flange is in the same plane as the rest of the palate)
113: ? → 1
189: ? → 0
197: 0 → 1 (Simoes et al. 2018 score the dorsal process of the coronoid as absent (0). However, Carroll (1981 p.348) notes that a small triangular coronoid extends above the margin of the jaw (also see Carroll 1981 Fig.12))
207: ? → 0

Youngina:
Data sources – Literature: Romer 1956, Gow 1975, Carroll 1981, Ezcurra 2016. Specimens examined – BP/1/70, 2614, 2871, 3859, FMNH UC 1528

3: 1 → 0 (Simoes et al. 2018 score a posterodorsal process of the premaxilla as present (1). However, although Gow (1975 Fig1) does show a small process of the premaxilla that seems to overlay the subnarial process of the maxilla in BP/1/2871, upon examination of this specimen this morphology is not evident. Further, a slight overlay is not homologous with the posterodorsal process in other taxa scored as (1), where the process extends posterior to the external naris and prevents contact between the eternal naris and the maxilla)
10: 0 → ? (Simoes et al. 2018 score the septomaxilla as present (0). However, Gow (1975) notes that the details of this bone are totally lacking. In Carroll's reconstruction of the skull of *Youngina* (1981 fig 9) the septomaxilla is represented, however, it is not identifiable in any of the examined specimens)
11: 1 → ? (The position of the septomaxilla relative to the nasal capsule cannot be determined (see above))
48: 0/1 → 0
89: ? → 1
113: ? → 1
115: ? → 0
116: ? → 0
128: 0/1 → 0
140: ? → 0
172: ? → 1
275: 1 → ? (Simoes et al. 2018 score the supraglenoid foramen as present (1). In BP/1/3859, the only example of a scapulocoracoid in *Youngina*, the area around the glenoid facet is badly eroded, and although it does contain a small hole that may be mistaken for a supraglenoid foramen, the presence of a supraglenoid foramen is unclear. We agree with Ezcurra (2016), who scores this character as (?))
303: 1 → 0 (Simoes et al. 2018 score an emargination of the anterior border of the ischium as present (1) as a proxy for the thyroid fenestra. There is a small triangular shaped embayment of the anterior margin of the ischium in one specimen of *Youngina* (BP/1/3859). Gow (1975) notes that the notch may indicate an incomplete ossification of the ischium and pubis, and refers this to Romer (1956 p.318).

Romer notes of the pubo-ischial plate, "primitively the ventral margin of the plate formed a nearly straight line. In incompletely ossified specimens there may be a notch or indentation at the suture between the pubis and ischium". In BP/1/3859, the ventral margin is more or less complete and would have met in a straight line with the pubis (although the specimen only has the left pubis and right ischium). Both specimens have been examined in close detail and the notch in both elements is clearly bordered by incomplete bone. We therefore agree with Romer that this is not homologous with the thyroid fenestra and the pubo-ischial plate is incomplete in BP/1/3859)

Acerosodontosaurus:
Data sources – Literature: Currie 1981, Bickelmann et al. 2009. Specimens examined: MNHN 1908-32-57

32: 0 → ? (Simoes et al. 2018 score ornamentation on the lateral surface of the prefrontal as absent (0). However, we consider the natural mould of lateral surface of the prefrontal in MNHN 1908-32-57 is too poorly preserved to determine the presence or absence of ornamentation)
33: 1 → ?
38: 0 → ? (Simoes et al. 2018 score the quadratojugal as present (0). Bickelmann et al. (2009) note that the quadratojugal identified by Currie (1981) is a fragment of rib head, and that the quadratojugal is not preserved)
39: 0 → ? (Simoes et al. 2018 score the anterior process of the quadratojugal as present (0). Since the quadratojugal is unknown (see above), we cannot determine whether or not an anterior process was present)
176: ? → 1
177: ? → 0
190: 0 → 1(Simoes et al. 2018 score the retroarticular process as absent (0). However, Bickelmann et al. (2009 p.655) note the presence of an elongated, tapering retroarticular process)
191: - → ?
192: - → ?
195: - → ?
300: ? → 1
301: ? → 1

Coelurosauravus jaekeli:
Data sources: Literature: Evans and Haubold 1978, Bulanov and Sennikov 2015.

27: 1 → 0 (Simoes et al. 2018 score the lacrimal as absent (1). Evans and Haubold (1978 p.278) suggest a small bone mass ventral to the orbital region of the prefrontal may be a small lacrimal. In addition, Bulanov and Sennikov (2015 p.419) also note a rudimentary lacrimal was probably present in *C. elivensis* – see below)
70: 0 → - (since the subolfactory processes are scored as absent (Simoes et al. 2018 c.69), the absence or presence of fusion between them should therefore be scored as inapplicable)

Coelurosauravus elivensis:
27: ? → 0
70: 0 → - (since the subolfactory processes are scored as absent (Simoes et al. 2018 c.69), the absence or presence of fusion between them should therefore be scored as inapplicable)

Utatsusaurus:
Data source: Literature: Cuthbertson et al. 2013

107: 0 → 1 (Simoes et al. score the transverse process of the pterygoid as absent (0). Cuthbertson et al. (2013 p.823) note that a transverse process is present on the pterygoid)
108: - → 1

Tanystropheus:
70: 0 → - (since the subolfactory processes are scored as absent (Simoes et al. 2018 c.69), the absence or presence of fusion between them should therefore be scored as inapplicable)

Langobardisaurus:
Data sources – Literature: Dilkes 1998, Renesto 1994

36: ? → 1
70: 0 → - (since the subolfactory processes are scored as absent (Simoes et al. 2018 c.69), the absence or presence of fusion between them should therefore be scored as inapplicable)
355: 0 → 1 (Renesto (1994 figs 7 and 8) shows the pedal lateral centrale as present, and Dilkes (1998) scores it as present, contacting the tibia)

Macrocnemus fuyuanensis:
Data source – Literature: Jiang et al. 2011

28: 2 → 1 (This character has been changed to a binary character since the revision of the taxon list rendered state (2) as uninformative. In addition, the lacrimal is anteriorly placed in relation to the prefrontal in *M. fuyuanensis* (see Jiang et al. 2011))

Prolacerta:
Data sources: Literature – Gow 1975, Evans 1986, Modesto and Sues 2004, Spiekman 2018.
Specimens examined – BP/1/471, 2675, 4504, 5066, 5375, 5880.

60: 0/1 → 1
69: 1 → ? (This character describes a ventral extension of the crista cranii (subolfactory processes), as per Gauthier et al. 2012 c.38. Simoes et al. 2018 score this as present in *Prolacerta*. We are unable to find any evidence of this morphology on the specimens of *Prolacerta* examined, or in the literature. We therefore consider this uncertain)
70: 0 → ? (Simoes et al. 2018 score for the absence of fusion of the subolfactory processes (c.69). Since we consider the presence of these processes uncertain, we consequently score this character as (?))
73: 0 → 0/1 (Simoes et al. 2018 score the pineal foramen as present (0). The pineal foramen is distinctly polymorphic in *Prolacerta* specimens. For example, it is absent or reduced to a small scar in BP/1/471. This variation was noted by Modesto and Sues (2004) and they further note the foramen is entirely absent in UCMP 37151)
115: ? → 0
116: ? → 0
121: 1 → 0 (Simoes et al. 2018 score the quadrate conch as present (1) in *Prolacerta*. However, Modesto and Sues (2004 p.344) note that "the tympanic crest resembles that of lepidosauromorphs except for the absence of a conch". Also, the right quadrate in BP/1/5375 shows no sign of a conch.)
157: 0 → 1 (Simoes et al. 2018 score the laterosphenoid as absent (0). A recent scan of the braincase of *Prolacerta* has however provided evidence that the laterosphenoid is present (pers. comm. G. Viglietti 2020))
297: 0 → 1 (Simoes et al. 2018 score the supraacetabular buttress as absent (0) in *Prolacerta*. However, A supraacetabular buttress is present on the ilium of BP/1/2676 (see Spiekman 2018 Fig.11)

311: 1 → 0 (Simoes et al. 2018 score the pectoral process of the humerus as absent (1) in *Prolacerta*. However, Spiekman (2018) notes that the deltopectoral crest of both humeri of UWBM 95529 are present. This incorporates the pectoral process of the humerus, which connects the deltoid process to the humeral head (Simoes et al 2018 remarks). Therefore, the pectoral process is herein scored as present (0))
312: - → 1 (see above in respect to the connection of the pectoral process to the humeral head)
321: ? → 1

Megalancosaurus:
Data sources; Literature – Renesto 1994, 2000, Renesto and Della Vecchia 2005, Castiello et al. 2016.

3: 1 → 0 (Simoes et al. 2018 score a posterodorsal process of the premaxilla as present (1). However, the overlay is minimal, and is not homologous with the posterodorsal process in other taxa scored as (1), where the process extends posterior to the external naris and prevents contact between the eternal naris and the maxilla)
27: ? → 0
342: ? → 0

Askeptosaurus:
Data source: Literature – Müller 2004. Specimens examined – MSNM V456

327: 1 → 0 (Simoes et al. 2018 scores the internal trochanter of the femur as absent (1). However, Müller (2004 p. 1359) suggests that a modest expansion on the medial edge of the proximal surface of the femur in MSNM V456 may be the internal trochanter. Our examination of this specimen concurs with this view)

Philydrosaurus:
41: 2 → 1 (This character has been modified to binary states – see note on c.41 above)

Champosaurus:
41: 2 → 1 (This character has been modified to binary states – see note on c.41 above)

Teyumbaita:
70: 0 → - (since the subolfactory processes are scored as absent (Simoes et al. 2018 c.69), the absence or presence of fusion between them should therefore be scored as inapplicable)

Hyperodapedon:
70: 0 → - (since the subolfactory processes are scored as absent (Simoes et al. 2018 c.69), the absence or presence of fusion between them should therefore be scored as inapplicable)

Trilophosaurus:
Data source: Spielman et al. 2008

27: 1 → 0 (Simoes et al. 2018 score the lacrimal as absent (1). However, Spielman et al. (2008 p.30) describe the lacrimal in some detail)
38: ? → 0
70: 0 → - (since the subolfactory processes are scored as absent (Simoes et al. 2018 c.69), the absence or presence of fusion between them should therefore be scored as inapplicable)

Proterosuchus alexanderi:
Data sources: Literature – Modesto and Sues 2004, Ezcurra 2016

70: 0 → - (since the subolfactory processes are scored as absent (Simoes et al. 2018 c.69), the absence or presence of fusion between them should therefore be scored as inapplicable)
154: 0 → 1 (Simoes et al. 2018 score the medial contact of the exoccipitals as absent (0). However, Modesto and Sues (2004 p.344) note that the exoccipitals meet medially in *Proterosuchus*. Further, Ezcurra (2016 c.211) scores both *P. alexanderi* and *P. fergusi* as medial contact of the exoccipitals present)

Proterosuchus fergusi:
Data sources: Literature – Modesto and Sues 2004, Ezcurra 2016

70: 0 → - (since the subolfactory processes are scored as absent (Simoes et al. 2018 c.69), the absence or presence of fusion between them should therefore be scored as inapplicable)
154: 0 → 1 (Simoes et al. 2018 score the medial contact of the exoccipitals as absent (0). However, Modesto and Sues (2004 p.344) note that the exoccipitals meet medially in *Proterosuchus*. Further, Ezcurra (2016 c.211) scores both *P. alexanderi* and *P. fergusi* as medial contact of the exoccipitals present)

Euparkeria:
Data source: Literature – Sobral et al. 2016

135: 1 → 0 (Simoes et al. 2018 score the vidian canal as fully enclosed (1). However, there is no closure of the vidian sulcus prior to the entry foramen on the ventral surface of the parabasisphenoid (see Sobral et al. 2016 figs. 11a and 12f))

Cyamodus:
38: ? → 0
329: 0 → ? (Simoes et al. 2018 score the intertrochanteric fossa as present (0) in this character. However, they also score the internal trochanter as absent (1) in c.327. We feel that the presence of the fossa is uncertain given the absence of the trochanter)

Placodus:
Data source: Literature – Neenan et al. 2012

70: 0 → - (since the subolfactory processes are scored as absent (Simoes et al. 2018 c.69), the absence or presence of fusion between them should therefore be scored as inapplicable)
124: 0 → 1 (Simoes et al. 2018 score the position of the carotid foramen into the braincase as in the lateral wall (0). However, the entrance is ventral in *Placodus gigas* (see Neenan et al. 2012))

Serpianosaurus:
70: 0 → - (since the subolfactory processes are scored as absent (Simoes et al. 2018 c.69), the absence or presence of fusion between them should therefore be scored as inapplicable)
113: 1 → ? (Simoes et al. 2018 score the ectopterygoid as present (1). However, Rieppel (1989 p.13) notes that the presence of the ectopterygoid cannot be unequivocally established, and it is probably absent. We therefore consider this state as uncertain)

Kuehneosaurus:
Data sources: Robinson 1962, 1967; Pamela Robinson unpublished manuscript notes; holotype of *Kuehneosaurus latus* BMNH R.8172; holotype of *Kuehneosuchus latissimus* BMNH R.6111; isolated cranial and postcranial elements: BMNH R. 6001, 6003, 6004, 6112- 6115, 12647, 12861, 12864, 12866-12871, 12874, 12877, 12879, 12880, 12885, 12890, 12894-12896, 12900, 12903, 12904, 12983,

12991, 12925 (as figured in Evans 2009); a large collection of isolated bones in the collections of the Natural History Museum, London, without formal BMNH catalogue numbers. Note that Robinson originally described all material of the British gliding reptile under the name *Kuehneosaurus*, as *K. latus* and *K. latissimus*. However, she subsequently moved *K. latissimus* into a new genus *Kuehneosuchus latissimus* but this designation is based on postcranial characters, with no cranial features described. Most other elements in the collection at the NHM are simply labelled *Kuehneosaurus*. Thus *Kuehneosaurus* herein should be considered as referring broadly to UK kuehneosaurs. The changes to scoring are based on a combination of personal observations of specimens by SEE, details from unpublished figures, and from unpublished manuscript notes by P.L. Robinson.

8: ? → 1
16: ? → 1
20: ? → 1
21: ? → -
23: ? → 0
24: ? → -
25: ? → 1
26: ? → 0
32: 1 → 2 (Tubercles present along orbital margin)
38: 1 → ? (Changed to ? as there is a possibility of quadratojugal being fused to ventral edge of conch, e.g. in BMNH R12895, Evans 2009, Fig. 15C)
39: - → ? (Changed from inapplicable to ? due to scoring of c.38)
40: - → 0 (as above)
41: - → ? (as above)
42: - → 0 (There is no foramen)
48: ? → 1 (A concavity is present (Evans 2009, Fig.12))
59: 2 → 3 (Given the arrangement of the facet for the postfrontal on the frontal, rather than the parietal, we interpret this position as largely anterior)
62: 0 → ? (As there is no articulated material, there is no certainty that a supratemporal was absent)
63: - → ? (Scored due to coding changed in c.62)
64: ? → 1 (There are no facets on the parietal that could accommodate a tabular)
65: ? → 1 (There are no facets on the parietal that could accommodate postparietals)
66: ? → - (Non-applicable due to change in coding for c.65)
70: 0 → - (There are no subolfactory processes, only thickened cristae crania, so this is inapplicable)
73: 0 → 1 (There is no parietal foramen in kuehneosaurs – the reconstruction given by Robinson simply interprets a foramen at the frontoparietal border because there is a slight gap in the midline and the author (PLR) expected a foramen should be present.)
75: - → 0 (The parietals have a short supratemporal process that is single so cannot be inapplicable)
76: 0 → 1 (In mature specimens there are rugosities on the parietal (e.g. Evans 2009, Fig.8D))
86: 1 → 0 (There are no parasagittal crests on the kuehneosaur parietal – just a sharp right angle from dorsal to lateral margin)
97: ? → 1
98: ? → 0
99: ? → 0
100: ? → 1
101: ? → 0
102: - → 0 (The palatine shows no palatine foramen)
103: - → ? (The region is not well enough preserved on existing specimens)
104: - → 0 (The shelf is absent)
106: ? → 0

113: ? → 1
123: ? → 0
124: 0 → 1 (The carotid arteries perforate the ventral surface of the sphenoid, not the lateral surface)
125: 0 → ? (This region is insufficiently known in existing specimens)
137: ? → 0
149: 0 → 1 (There is no crista interfenestralis in *Kuehneosaurus* because there is no lateral opening of the recessus scala tympani as the metotic fissure is undivided)
152: 0 → - (The exoccipitals contribute to the occipital condyle but they tend to fuse with the basioccipital, e.g. AMNH 7770)
165: ? → 0
166: ? → 0
167: ? → 1
168: ? → 1
172: 1 → 0 (There is no coronoid process of the dentary in *Kuehneosaurus)*
173: 0 → - (This is inapplicable given the score of c.172)
174: ? → - (as above)
175: ? → 0
180: ? → 0
182: ? → 1
183: ? → 0
184: ? → 1
188: 0 → ? (The articular is sheathed by the prearticular in *Kuehneosaurus* but the degree of fusion is uncertain)
189: 0 → 1 (There is a foramen for the chorda tympani)
193: 1 → 0 (There is no medial process in *Kuehneosaurus*)
206: ? → 1
207: ? → 0
208: ? → 0
213: ? → 3
219: ? → 0
220: ? → 0
221: ? → 1
222: ? → 0
223: ? → 1
224: ? → 0
227: ? → 1
228: ? → 4
231: ? → 0
232: 0/1 → 0 (A crest (as opposed to a rounded midline ridge marking the position of the notochord) is absent)
237: ? → 0
238: ? → -
240: ? → 0
241: ? → -
243: ? → 0
244: ? → 0
260: ? → 0
265: ? → 1
266: ? → -
273: 0 → ? (The preservation of specimens is such that this character is uncertain)
276: 0 → 1 (There is a supraglenoid buttress)

280: 1 → 0 (There is no emargination of the scapulocoracoid in *Kuehneosaurus*, but the bone is slender – not the same thing)
286: 0 → ? (Calcified cartilage does not preserve in this fissure material, therefore this should be scored as uncertain)
287: ? → 0
288: ? → 0
290: ? → 0
291: ? → 0
292: ? → 0
293: ? → 0
294: ? → 0
295: ? → 1
297: 0 → 1 (There is a supra-acetabular buttress)
301: 0 → 1 (There is a pubic tubercle)
303: 1 → ? (There is uncertainty as to this feature in *Kuehneosaurus* – a small notch can simply be due to non-ossification at this point)
307: 1 → 3 (There is a complete ectepicondylar foramen)
310: 1 → 0 (There is a large capitellum)
314: ? → 0
316: 0 → ? (This region of the radius is poorly known in *Kuehneosaurus*)
327: 1 → 0 (There is an internal trochanter in *Kuehneosaurus*)
329: 1 → 0 (There is an intertrochanteric fossa in *Kuehneosaurus*)
332: ? → 0
334: ? → 1
338: ? → 1
340: ? → 0
341: ? → 0
342: 0 → 1 (Gastralia were present on the holotype of *Kuehneosaurus latus* (BMNH R.8172) although Robinson (in lit.) reported that many of them were removed when the specimen was prepared).

Icarosaurus:
Data source: Colbert 1966, 1970; specimen AMNH 2101; unpublished personal notes from P.L. Robinson; personal observations by SEE of holotype.

59: 2 → 3 (The articular facets on the frontals show that the postfrontal was mainly anterior to the parietal (e.g. Colbert 1966, Fig.6; Colbert 1970, Fig.7))
70: 0 → - (The frontals are seen in dorsal view only, but they are extremely shallow and given that the right bone has rotated over the left (e.g. Colbert 1966, Fig. 6; 1970, Fig.6), it is unlikely that there is a strong lateral ridge (crista crania) or subolfactory process that would limit this movement. It is therefore scored as inapplicable)
73: 0 → 1 (There is no evidence of a parietal foramen. Colbert (1970) says its presence 'cannot be established beyond all doubt' but reconstructs one between the frontal and parietal because of a possible midline gap between the frontals, possibly influenced by Robinson's reconstruction of *Kuehneosaurus*)
75: - → ? (This is not inapplicable because there are at least short supratemporal processes (partially hidden at their tips by overlying bones e.g. Colbert 1070, Fig.6))
228: 0/3 → 4 (The vertebral centra are described by Colbert (1966) as amphicoelous, but they are not notochordal, so amphiplatyan is a closer description)
280: 1 → 0 (The scapula blade appears slender (although Colbert, 1966, describes it as 'rather broad and blade-like') but there is no evidence that it is emarginated)

300: 0 → ? (The blade of the pubis is not well preserved and Colbert's sketch (1966, Fig. 10) does not match the shape of the bone in his photographic image (1966, Fig. 9). It is therefore preferable to code this character with (?))
301: 0 → ? (As above. There is a distinct angulation on the anterior margin of the pubis (e.g. as seen in Colbert 1970, Fig.12) that is not shown his (1970, Fig.13) line drawing of the bone)
342: 0 → ? (The only known specimen is preserved in dorsal view precluding a view of the anteroventral region of the abdomen. It is therefore not possible to determine whether gastralia were present. Given they were present in *K. latus*, it is likely they were also present in *Icarosaurus* but it is scored conservatively as (?))

Pamelina:
Data source: Evans 2009; Specimens in the collections of the Institute of Paleobiology, Polish Academy of Sciences, Warsaw (ZPAL); holotype maxilla ZPAL RV/1036; and a large collection of isolated skull and postcranial elements including ZPAL RV/143, 144, 147, 157, 378, 383, 384, 387,441, 451, 555, 612, 617, 627, 936, 975, 979, 981, 1003, 1004, 1008, 1011, 1013,10151027,1029, 1034-1036, 1039, 1042,1043, 1046, 1047, 1048, 1049, 1066, 1067, 1072, 1077, 1081,1082, 1128, 1194, 1197, 1199, 1203, 1204, 1205, 1208, 1211, 1214, 1215, 378, 381, 383-384, 387, 537

18: ? → 0
20: ? → 1
21: ? → -
27: ? → 0
34: 0 → ? (As the material is all disarticulated this is unknown)
38: 1 → ? (There is a notch in the margin of the quadrate resembling that of taxa with a quadratojugal foramen. The presence or absence of a quadratojugal is therefore uncertain (Evans 2009))
39: - → ?
40: - → ?
41: - → ?
42: - → ?
59: 2 → 3 (Given the position of the postfrontal facet on the frontal rather than the parietal, its medial margin lies anterior to the parietal (Evans 2009))
64: ? → 1
70: 0 → - (There are no subolfactory processes – only shallow cristae crania. The character is therefore inapplicable)
73: ? → 1 (There is no parietal foramen in *Pamelina*)
78: 0 → 1 (There are tabs from the parietals underlying the frontal)
123: ? → 0 (Although the tip of the quadrate is damaged in specimens of *Pamelina*, the narrow cephalic condyle, and the morphology of the squamosal itself, shows that there is not a notch for the squamosal as in the typical squamate joint)
137: 0 → 1 (The dorsum sella is present (Evans 2009, Fig 17))
148: ? → 0 (The morphology of the parasphenoid rostrum shows that an orbitosphenoid process cannot have been present)
150: 0 → ? (As no exoccipitals are recognised for this taxon, this should be (?))
151: 0 → ? (As above)
152: 1 → ? (As above)
153: 0 → ? (As above)
154: 0 → ? (As above)
208: ? → 0
228: ? → 0

229: ? → 1
230: ? → 0
231: ? → 0
232: ? → 0
233: ? → 0
236: ? → 0
247: ? → 0
248: ? → 0
249: ? → -
251: ? → 0
252: ? → 0
253: ? → 0
254: ? → 0
255: ? → 0
256: ? → 0
257: ? → 0
258: ? → 0
260: ? → 0
266: ? → 1
268: ? → 1
269: ? → 1
270: ? → 1
297: ? → 1
298: ? → 0
299: ? → 0

Megachirella:
Data source: Renesto & Posenato (2003), Renesto & Bernardi 2014, Simoes et al. 2018. Type and only specimen, PZO 628 Museo di Scienze Naturali dell 'Alto Adige, Bolzano, Italy.
The specimen has been redescribed (Simoes et al. 2018) based on CT scans but appears very compressed. Several characters appear to be too poorly preserved to code and these have been changed to (?) below.

18: 0 → ? (Preservation too poor)
47: 1 → ? (Simoes et al. (2018) have a POF labelled on the right but crushed into level of palate. Renesto & Bernardi (2014, Fig.3) show a short ventral process reaching the jugal on this side)
59: 2 → ? (As above – this POF element lies medial to the coronoid process and the jugal lies lateral to the coronoid, so the original position of this element is uncertain. Renesto & Bernardi's (2014, Fig.3) suggests the postfrontal-postorbitofrontal lies mostly anterior to the parietal)
67: 1 → ? (Only part of the frontal is preserved. It is probably but not certainly fused)
72: 1 → ? (It is unclear whether the parietals are fused (Simoes et al. 2018) or paired (Renesto & Bernardi 2014))
73: 0 → ? (A parietal foramen is coded as present (Simoes et al. 2018, Fig.1) but it is not labelled and it is not obvious where it is supposed to be. It does not appear in Renesto & Bernardi (2014))
97: ? → 1 (Simoes et al. 2018 figure (Fig.1e) of the palate shows palatal tooth rows running forward from the pterygoid into the region identified as palatine)
106: 0 → ? (Given the poor preservation of the anterior end of the pterygoid, this should be (?))
109: 0 → ? (The poor preservation of this region makes it difficult to code with confidence)
122: 1 → 0 (There is no hook-like suprastapedial process (Simoes Fig. 1d))

123: 1 → 0 (The squamosal appears to sheath the top of the quadrate – this is not equivalent to the peg and notch arrangement in a squamate)
142: 1 → 0 (The structure labelled (Simoes et al. Fig.1f) seems to be the ridge of the anterior semi-circular canal – not a separate alar process)
150: 0 → ? (The poor preservation of this region makes it better to code as (?))
151: 0 → ? (The exoccipital is not labelled in Simoes et al. (2018) figure of the braincase, making it difficult to confirm this coding)
170: 0 → ? (As the lingual surface is covered by the splenial, this feature is not visible and it is not shown in the section of the jaw (Simoes et al. Fig. 1g))
179: ? → 3
198: 0 → 1
200: 1 → ? (This cannot be confirmed on the images shown in Simoes et al. (2018, Fig.1))
201: 0 → ? (This cannot be confirmed on the images shown in Simoes et al. (2018, Fig.1))
206: 1 → ? (The dentition is not preserved well enough to score this confidently)
216: ? → 0
217: 0 → ?
272: 0 → ? (The mode of preservation is not good enough to determine whether this cartilaginous/mineralised cartilage structure is present)
273: 0 → ? (As above)
287: 1 → ? (Given the compression of this region this should be coded as (?))
289: 0 → ? (As above)
323: 0 → ?

Sophineta:
Data source; Evans & Borsuk-Białynicka 2009; specimens in the collections of the Institute of Paleobiology, Polish Academy of Sciences, Warsaw (ZPAL); holotype ZPAL RV/175, maxilla and a large collection of referred cranial and postcranial elements including ZPAL RV/3,7,10, 13, 23, 174-178, 189, 226-249, 392, 443, 445, 455, 472, 493, 627-628, 823-824, 948-950, 952, 959, 965-974,1053-1059, 1061-1063, 1069, 1079-1080, 1086, 1098,1101, 1108, 1110, 1121. Simoes et al. (2018) did not score postcranial characters as described in Evans & Borsuk-Białynicka (2009), presumably questioning their attribution. However, the size and morphology of these elements would preclude their attribution to any of the other small reptiles in the Czatkowice assemblage. These characters(from 228 onward) have therefore been scored herein.

32: ? → 0 (There is no sculpture on the preserved parts of attributed prefrontals)
45: ? → 0 (The position of the facets on postorbital and postfrontal suggests the postorbital lies mainly lateral to the postfrontal)
64: ? → 1 (Neither squamosals nor parietals show any trace of a facet that might have accommodated a tabular)
76: 0 → 1 (The parietals are weakly sculptured with ridges and tuberosities)
78: 0 → 1 (Facets on the frontals imply the presence of parietal tabs)
118: ? → 0 (A small foramen pieces the quadrate pillar e.g in ZPAL RV/974)
123: ? → 0 (Although the tips of the quadrates are damaged, the morphology of the tip, and that of the squamosal, shows that the squamate 'peg-in'notch' arrangement cannot have been present)
172: ? → 0 (The morphology of the post-dental margin of the dentary, and the position of the long coronoid facet along this margin, argues against the presence of a coronoid process)
173: ? → 0 (There is no expansion of the post-dental ramus of the dentary)
174: ? → - (Given the absence of a process, this is inapplicable)
197: 1 → ? (In the absence of an attributed coronoid bone, this character is scored (?))
198: ? → 0 (The facet for the coronoid on the dentary is confined to the medial side of the dentary)
200: 1 → ? (As for 197 above)

201: 0 → ? (As for 197 above)
208: ? → 0 (The eroded bases of dentary teeth show that replacement was lingual)
228: ? → 0
229: ? → 0
230: ? → 1
231: ? → 1
232: ? → 0
233: ? → 0
234: ? → 0
236: ? → 0
243: ? → 0
244: ? → 0
246: ? → 0
247: ? → 0
248: ? → 0
249: ? → - (There are no zygosphenes developed on the vertebrae and the character is inapplicable)
251: ? → 0
252: ? → 0
253: ? → 0
255: ? → 0
256: ? → 0
257: ? → 0
258: ? → 0
269: ? → 1
270: ? → 1
296: ? → 0
297: ? → 1
298: ? → 1

Palaegama:
Data source: Carroll 1975, 1977; specimen No.3707 McGregor Museum (type and only specimen), Kimberley (personal observation, SEE, and cast of the type held at UCL)

18: ? → 0 (Prefrontal, maxilla/lacrimal contact one another anterior to the orbit (e.g. Carroll 1975, Fig.2))
19: ? → 0 (As above)
26: 0 → ? (The preservation of this region is not good enough to code this character)
47: ? → 1
48: - → 0
49: ? → 0
61: - → 0
64: ? → 1
68: 1 → ? (Preservation does not permit this to be coded)
71: 0 → ? (Preservation does not permit this to be coded)
78: 0 → ? (This is questionable as Carroll's figure (1975,Fig.2) suggests a tab may be present)
81: 1 → ? (Preservation does not permit this to be coded)
82: - → ? (Preservation does not permit this to be coded)
228: 0 → ? (The centra are probably amphicoelous but none seems to be preserved end on)
230: 0 → ? (Preservation does not permit this to be coded with assurance)
232: 1 → ? (There are rounded keels but these are not homologous to the keels on snakes)

233: - → ? (As the articular surfaces of the centra are not visible, and are obscured in ventral view by intercentra, this cannot be coded with certainty)
235: 2 → ? (Carroll (1975) describes 2 sacral ribs but the preservation of this region is poor with only one pair of ribs seen clearly)
236: 0 → ? (Most of the tail is missing)
263: 0 → ? (Very few of the rib heads are visible and intact)
264: 0 → ? (Very few of the rib heads are visible and intact)
268: 1 → ? (It is unclear in Carroll's figure (1975, Fig 1) whether the single exposed sacral rib is fused or sutured to the vertebral centrum)
273: 0 → ? (The preservation is not good enough to code this confidently)
287: 0 → ? (The clavicles are incompletely preserved)
289: 0 → ? (The clavicles are incompletely preserved)
298: 0 → ? (The preservation is not good enough to code this confidently)
301: 1 → ? (The preservation is not good enough to code this confidently)
304: 0 → ? (The preservation is not good enough to code this confidently)
306: 0 → ? (The preservation is not good enough to code this confidently)
310: 1 → ? (The preservation is not good enough to code this confidently)
316: 0 → ? (The preservation is not good enough to code this confidently)
319: 0 → ? (The preservation is not good enough to code this confidently)
327: 0 → ? (The preservation is not good enough to code this confidently)
328: 0 → ? (The preservation is not good enough to code this confidently)
329: 0 → ? (The preservation is not good enough to code this confidently)
330: 0 → ? (The preservation is not good enough to code this confidently)
331: 0 → ? (The preservation is not good enough to code this confidently)
342: 0 → ? (Carroll (1975) figures fragments of slender elements between the ribs (Fig.1) that are likely to be gastralia)

Gephyrosaurus:
Data source: Evans 1980, 1981; extensive collection of catalogued cranial and postcranial bones in the collections of the Natural History Museum London, and uncatalogued specimens at UCL and NHM. Material of the braincase, as described in Evans 1977 PhD thesis, provides extra scoring for braincase characters.

1: 0 → 0/1 (The premaxillae occasionally fuse in mature *Gephyrosaurus*)
9: 0 → 1 (The premaxilla of Gephyrosaurus has a posterior flange bearing a distinct facet for the vomer (e.g. Evans 1980, Fig.30))
16: ? → 1 (A superior alveolar foramen is present)
24: 2 → 1 (The ventrolateral flange of the nasal articulates with the anterior margin of the maxillary facial (=nasal) process. It therefore lies anterior to the maxillary process)
25: 0 → 1 (The nasals contain foramina (Evans 1980, Fig.5))
34: 0 → ? (Although it is unlikely that these bones were present, the fact that *Gephyrosaurus* is based on re-articulated isolated elements means it is preferable to code this as (?))
45: 1 → 0 (Postorbital dorsal margin lies mainly lateral to the postfrontal)
59: 2 → 3 (The postfrontal overlies the parietal at its articulation (i.e. dorsal) but most of the postfrontal medial margin lies against the frontal, anterior to the parietal, i.e. state (3))
61: 1 → 0 (The medial margin of the postfrontal has only a slight concavity and does not clasp a projecting frontoparietal expansion. It is therefore coded as (0))
64: ? → 1 (There are no facets on parietals or squamosals that could accommodate this element)
68: 0 → 1 (The facets on the anterior margin of the parietal suggest that the frontal had short posterior processes that overlapped the parietal laterally)
76: 3 → 1 (The parietal has ridges and concavities between them, not strictly pits)

78: ? → 1 (Facets on the anterior margin of the parietal suggest that the frontal and parietal slotted into each other, with a parietal shelf briefly underlapping the frontal)
86: 1 → 0 (There is no crest on the dorsolateral region of the parietal)
90: ? → 1 (The vomer is a thin element that is rarely preserved intact, but the facet on the premaxilla (see ch.9) shows that the vomer contacted the premaxilla)
98: ? → 0
99: ? → 0
102: ? → 0
103: ? → 1
106: ? → 0
110: ? → 1
111: ? → 1
112: ? → 0
123: 1 → 0 (There is no notch on the cephalic condyle of the quadrate – the facet for the squamosal extends along the upper margin of the quadrate tympanic crest (e.g. Evans 1980, Fig.17) and the articulation is like that of *Sphenodon* not squamates)
124: 0 → 1 (The carotid foramen is ventral not lateral. A lateral position occurs when the parasphenoid expands to close a vidian canal)
125: ? → 0 (Braincase material of *Gephyrosaurus* (unpublished except in thesis) shows no lateral ascending process)
126: ? → 0
127: ? → 0
128: ? → 0
129: ? → 0
131: ? → 0 (There are sufficient specimens of basioccipital to show that no epiphyses were present)
132: 0 → 1 (The basioccipital is fused to the exoccipitals (e.g. Evans, Fig. 37) in mature individuals)
152: 1 → - (Inapplicable as elements are fused)
157: ? → 0 (There are no laterosphenoids)
170: 0 → 0/1 (The development of the dorsal and medial margins of the Meckelian fossa is variable and there can be a short closure)
184: ? → 0 (There does not appear to be an anterior surangular foramen)
193: 0 →1 (There is a small tuberosity for pterygoideus (e.g. Evans 1980, Fig.45))
195: - → ? (As the prearticular and articular are fused, the contribution of the prearticular is not known)
200: 1 → 0 (The coronoid is almost completely medial on the lower jaw and bears a long posterior process)
201: ? → 0 (A short posteroventromedial flange is present (e.g. Evans 1980, Fig.43))
208: ? → 0 (This is the position of posterior replacements, i.e. (0) as lingual)
221: 0 → 1 (The atlas arch has postzygapophyses (Fig. 2, Evans 1981))
222: 1 → 0 (Atlas ribs present (0) as shown by rib tubercles on atlas intercentrum (Evans 1981, Fig. 2))
223: ? → 1 (Atlas pleurocentrum is fused to axis (Evans 1981, Fig. 3))
224: ? → 0 (Axis intercentrum is present and fused between the atlas pleurocentrum (odontoid process) and the axis pleurocentrum (Evans 1981, Fig.3))
225: ? → 0 (IC2 alone lies below the axis)
226: 0 → 1 (Axis IC fused to axis pleurocentrum (Evans 1981, Fig.3))
227: ? → 0 (There are rib tubercles on the axis intercentrum (Evans 1981, Fig. 3))
232: 1→ 0 (Posterior dorsal vertebral do not have a midventral crest – the rounded ridge is a typical feature of notochordal vertebrae – it does not constitute a crest)
235: ? → 2 9There are two sacral vertebrae)

237: ? → 1 (Cervical intercentra were present – as indicated by the recovery of isolated elements of both cervical intercentra (small crested) and dorsal intercentra (simple hemicircles) (Evans 1981, Fig.11))
238: ? → 0 (As there are no facets on the cervical centra, the intercentra were intercentral)
243: ? → 0 (Given the absence of any articular facets or haemapophyses on caudal vertebrae, the chevrons clearly articulated intervertebrally, as also indicated by the dorsal bar)
244: ? → 0 (They were clearly free as they are found complete in the fissure material)
252: ? → 0 (Are any cervical spines preserved well enough to show if there was a notch?)
262: ? → 0 (Many rib fragments have been recovered and there is no evidence of uncinate processes on any)
267: ? → 0 (There is no evidence of forking on preserved sacrals)
268: ? → 1 (They are evidently fused)
274: ? → 0 (There is no evidence for the presence of distal ribs and the curvature of the primary ribs would preclude it anatomically)

276: 0 → 1 (There is a supraglenoid buttress)
280: 1 → 0 (The scapula is not emarginated)
283: ? → 0 (There is no evidence of a procoracoid attachment)
284: ? → 0 (There is no coracoid emargination)
285: ? → 0 (There is no evidence of an articulation for a posterior coracoid)
291: ? → 0 (The clavicles end distally in a narrow tip that from the length of the clavicle in relation to the scapulocoracoid, and the orientation of the tip must have made contact with the anterior edge of the scapula blade)
295: 1 → ? (Although it is unlikely that a cleithrum was present, it is preferable to score this as (?))
297: 0 → 1 (There is a supra-acetabular buttress (Evans 1981, Fig. 17))
300: ? → 1 (The pubis has a complete obturator foramen (Evans 1981, Fig. 22))
301: ? → 1 (The pubis has a pubic tubercle (= pectineal process, Evans 1981 Fig.22))
314: ? → 1 (Epiphyses were present – as indicated by flat porous surfaces at the end of several limb bones where the epiphysis has detached (e.g. Evans 1981, Fig.19))
330: 0 → ? (The distal end of the tibia is incompletely preserved)
334: ? → 0 (The astragalus and calcaneum are fused in *Gephyrosaurus* and there is no foramen (Evans 1981, Fig. 27))
335: ? → 0 (The fusion of the astragalus and calcaneum precludes the presence of a pedal lateral centrale (Evans 1981, Fig. 27))
342: ? → 1 (Fragments are gastralia were recovered from the fissure deposits (Evans 1981, text))

Diphydontosaurus:
Data source: Whiteside 1981; uncatalogued articulated skeleton in the collections of PL Robinson (as deposited in the Natural History Museum, London); large collection of isolated postcranial specimens SEM scanned at UCL but undescribed. Characters 219 onward are therefore scored for the first time.

3: 1 → 0 (*Diphydontosaurus* does not have a posterodorsal process of the premaxilla (Whiteside 1981))
14: 1 → 0 (As in *Gephyrosaurus*, there is no obvious sutural surface for attachment of the maxilla (Whiteside 1981, Fig. 5); the anterior end of the maxilla has a small concavity that abutted the premaxilla (Whiteside 1981, Fig. 7))
61: 1 → 0 (As in *Gephyrosaurus*, the medial edge of the postfrontal is largely straight in *Diphydontosaurus* (Whiteside 1981, Fig. 12))
78: 0 → ?
86: 1 → 0 (Unclear from Whiteside's figure whether tabs are present or not)

123: 1 → 0 (There is no notch on the cephalic condyle of the quadrate that corresponds to the articular complex in squamates. The quadrate sits against a shelf on the squamosal as it does in *Sphenodon* and *Gephyrosaurus* (Whiteside 1981, Figs 17, 18))
124: 0 → 1 (In the absence of a closed vidian canal, the internal carotid enters ventrally (Whiteside 1981, Fig. 27))
219: ? → 1
220: ? → 0
221: ? → 1
222: ? → 1
223: ? → 1
226: ? → 0
228: ? → 0
229: ? → 0
230: ? → 1
232: ? → 0
234: ? → 0
235: ? → 2
236: ? → 1
242: ? → 0
243: ? → 0
244: ? → 0
245: ? → 2
246: ? → 0
247: ? → 0
248: ? → 0
249: ? → -
250: ? → -
252: ? → 0
253: ? → 0
255: ? → 0
256: ? → 0
257: ? → 0
258: ? → 0
259: ? → 0
260: ? → 0
262: ? → 0
263: ? → 0
264: ? → 0
268: ? → 1
274: ? → 0
296: ? → 1
297: ? → 1
299: ? → 0
400: ? → 1
301: ? → 1
302: ? → 0
303: ? → 1
305: ? → 1
308: ? → 0
313: ? → 0
315: ? → 0

326: ? → 0
328: ? → 0
331: ? → 1
332: ? → -
334: ? → 0
340: ? → 1
343: ? → 0
344: ? → -
345: ? → 0
346: ? → 0
347: ? → 0

Planocephalosaurus:
123: 1 → 0

Clevosaurus:
123: 1 → 0

Trioceros:
70: 0 → -
329: 0 → ?

Xantusia:
70: 0 → -

Plestiodon:
119: 0 → 1

Mabuya:
36: 0 → 1

Cordylus:
13: 1 → 0
119: 0 → 1

Broadleysaurus:
119: 0 → 1

Timon:
119: 0 → 1

Lacerta:
119: 0 → 1

Meyasaurus:
86: 1 → 0

Teius:
119: 0 → 1

Slavoia:

70: 0 → -

Gobinatus:
70: 0 → -
119: 0 → 1

Gilmoreteius:
119: 0 → 1

Petracola:
119: 0 → 1

Eichstaettisaurus:
119: 0 → 1

Huehuecuetzpalli:
86: 1 → 0

Dalinghosaurus:
119: 0 → 1

Lanthanotus:
119: 0 → 1

Pontosaurus:
86: 1 → 0

In the original dataset of Simões *et al.* (2018) eight characters were parsimony uninformative (c.19, c.112, c.160, c.177, c.180, c.196, c.209, c.285, c.346). The changes detailed above resulted in seven characters .(c.19, c.53, c.155, c.302, c.312, c.317, c.328) with non-variable scoring and these characters are therefore excluded from the Bayesian analysis. Nine characters were parsimony uninformative (c.10, c. 112, c.160, c.177, c.180, c.196, c.209, c.285, c.346). All characters have been retained in the matrix to inform future studies.

Optimisation of character states at key nodes for MCC tree

Lepidosauromorpha:

Unambiguous -
42 0 → 1
50 0 → 1
68 0 → 1
201 1 → 0

Acctran -
67 0 → 1
98 0 → 1
213 2 → 0
219 0 → 1

221 0 → 1
236 0 → 1
237 0 → 1
239 0 → 1
240 0 → 1
271 0 → 1
273 0 → 1
286 0 → 1
293 0 → 1
304 0 → 1
314 0 → 1
322 0 → 1
331 0 → 1
333 1 → 0
334 1 → 0
335 1 → 0
336 0 → 1
338 1 → 0
340 0 → 1
341 0 → 1
344 0 → 1
354 0 → 1
361 0 → 1

Deltran –
167 0→1
303 0→1
352 0→1
360 0→1
370 0→1

***Marmoretta + Fraxinisaura*:**

Unambiguous –
20 0→1
73 0→1
101 0→1

Acctran –
8 0 → 1
81 1 → 0
82 0 → 1
85 1 → 0
120 1 → 0
121 1 → 0
181 2 → 0
189 1 → 0
190 1 → 0
200 1 → 0
221 0 → 1
292 0 → 2

296 1 → 0
307 3 → 0

Deltran –
229 0 → 1
293 0 → 1
354 0 → 1

Lepidosauria:

Unambiguous –
69 0 → 1
231 0 → 1
298 0 → 1

Acctran –
45 1 → 0

118 1 → 0
188 0 → 1
229 1 → 0
371 0 → 1

Deltran –
81 0 → 1
98 0 → 1
109 1 → 0
120 0 → 1
121 0 → 1
219 0 → 1
237 0 → 1
239 0 → 1
240 0 → 1
271 0 → 1
286 0 → 1
314 0 → 1
322 0 → 1
334 1 → 0
335 1 → 0
336 0 → 1
338 1 → 0
340 0 → 1

Rhynchocephalia:

Unambiguous –
55 0 → 1
59 2 → 1
111 0 → 1
114 0 → 1
173 0 → 1

176 1 → 0
182 0 → 1
362 0 → 1
363 0 → 1

Acctran –
25 0 → 1
62 1 → 0
92 0 → 1
188 1 → 2
210 0 → 1
211 0 → 1
293 1 → 0
354 1 → 0
359 0 → 2
364 0 → 1

Deltran –
23 0 → 1
188 0 → 2
310 0 → 1
333 1 → 0

Squamata (total group):

Unambiguous –
61 0 → 1

Acctran –
36 1 → 0
89 1 → 0
95 0 → 1
116 0 → 1
124 1 → 0
125 0 → 1
151 0 → 1
162 0 → 1
168 1 → 0
226 0 → 1
265 0 → 1
272 0 → 1
288 0 → 1
291 0 → 2
310 1 → 0
324 0 → 1
349 1 → 0

Deltran –
354 0 → 1

Squamata excluding *Sophineta*:

Unambiguous –
50 1 → 0
198 0 → 1

Acctran –
7 0 → 1
21 0 → 1
27 0 → 1
45 0 → 1
68 1 → 0
71 0 → 1
118 0 → 1
170 0 → 1
229 0 → 1
348 1 → 0
349 0 → 2

Deltran –
324 0 → 1

Squamata excluding *Sophineta* and *Megachirella*:

Unambiguous –
38 0 → 1
123 0 → 1
227 0 → 1
284 0 → 1
342 1 → 0
356 0 → 1
357 0 → 1
367 0 → 1

Acctran –
85 1 → 0
97 1 → 0
105 1 → 0
135 0 → 1
138 0 → 2
142 0 → 1
171 0 → 1
316 0 → 1
352 1 → 0
364 0 → 1
369 1 → 2
371 1 → 0

Deltran –
27 0 → 1
36 1 → 0
188 0 → 1
236 0 → 1

265 0 → 1
273 0 → 1
348 1 → 0
361 0 → 1

Squamata (crown group):

Unambiguous –
1 0 → 1
83 0 → 1
348 0 → 2

Acctran –
43 0 → 1
49 0 → 1
67 1 → 0
73 0 → 1
352 0 → 1
359 0 → 1
369 2 → 1

Deltran -
71 0 → 1
89 1 → 0
95 0 → 1
97 1 → 0
105 1 → 0
116 0 → 1
124 1 → 0
125 0 → 1
162 0 → 1
272 0 → 1
288 0 → 1
293 0 → 1
305 1 → 0
309 1 → 0
330 0 → 1
333 1 → 0
341 0 → 1
364 0 → 1